

1 **Title**

2 **MafF is an anti-viral host factor that suppresses transcription from Hepatitis B Virus**
3 **and Epstein Barr Virus promoters**

4
5 **Running title**

6 **MafF restricts viral replication**

7 **Authors**

8 Marwa K. Ibrahim^{1,2}, Sameh A Gad^{1,3,4}, Kosho Wakae¹, Masaya Sugiyama⁵, Masataka
9 Tsuge⁶, Masahiko Ito⁷, Koichi Watashi¹, Xin Zheng¹, Takayuki Murata⁸, Mohamed El-
10 Kassas⁹, Takanobu Kato¹, Asako Murayama¹, Tetsuro Suzuki⁷, Kazuaki Chayama⁶, Kunitada
11 Shimotohno⁵, Masamichi Muramatsu^{1#}, Hussein H. Aly^{1#}, Takaji Wakita¹

12 **Affiliation**

13 ¹Department of Virology II, National Institute of Infectious Diseases, 1-23-1 Toyama,
14 Shinjuku-ku, Tokyo 162-8640, Japan

15 ²Department of Microbial Biotechnology, Division of Genetic Engineering and
16 Biotechnology Research, National Research Centre, 33 EL Bohouth St. (formerly El Tahrir
17 St.), Dokki, Giza, P.O. 12622, Egypt

18 ³Department of Biomedical Chemistry, Graduate School of Medicine, The University of
19 Tokyo, Tokyo, Japan

20 ⁴Department of Microbiology and Immunology, Faculty of Pharmacy, Minia University,
21 Minia, Egypt

22 ⁵Genome Medical Sciences Project, National Center for Global Health and Medicine, 1-7-1
23 Kohnodai, Ichikawa, Chiba, 272-8516, Japan

24 ⁶Department of Gastroenterology and Metabolism, Graduate School of Biomedical and
25 Health Science, Hiroshima University, 1-2-3 Kasumi, Minami-ku, Hiroshima, 734-8551,
26 Japan

27 ⁷Department of Virology and Parasitology, Hamamatsu University School of Medicine, 1-
28 20-1 Handayama, Higashi-ku, Hamamatsu, Shizuoka, 431-3192, Japan

29 ⁸Department of Virology and Parasitology, Fujita Health University School of Medicine,
30 Toyoake, Aichi 470-1192, Japan.

31 ⁹Endemic Medicine Department, Faculty of Medicine, Helwan University, Cairo, P.O. 11795,
32 Egypt

33 **Corresponding Authors**

34 Hussein H. Aly, email: ahussein@nih.go.jp

35 Masamichi Muramatsu, email: muramatsu@nih.go.jp

36

37 **Abstract**

38 Herein, we report that Maf bZIP transcription factor F (MafF) promotes host defense against
39 infection with Hepatitis B virus (HBV). Suppression of MafF increased HBV pre-genomic
40 RNA in HBV-infected primary hepatocytes. MafF inhibited the binding of the transcriptional
41 activator, HNF-4 α , at overlapping recognition sites in HBV core promoter. Mutations
42 introduced at the MafF binding site abolished the physical interaction between MafF and the
43 HBV promoter and counteracted MafF-mediated suppression of HBV replication. MafF
44 expression was induced by IL-1 β and TNF- α in an NF- κ B-dependent manner. These findings
45 are consistent with the identified induction of MafF expression in chronic HBV patients,
46 notably during the immune clearance phase. Interestingly, MafF also suppressed expression
47 of the trans-activator, BZLF1, that promotes lytic reactivation of Epstein Barr virus (EBV)
48 infection. In conclusion, MafF is a novel anti-viral host factor which is inducible by
49 inflammatory cytokines, and suppresses transcription from the promoters of susceptible DNA
50 viruses.

51

52

53

54

55

56

57

58

59

60

61

62

63

64

65

66 **Introduction**

67 In the earliest stages of viral infection, the host initially detects and counteracts infection via
68 induction of innate immune responses (1). Host restriction factors are essential components
69 of the innate antiviral immune response; these factors serve critical roles in limiting virus
70 replication before the adaptive immune response engages to promote virus clearance (2).
71 These anti-viral restriction factors are typically induced by cytokines, including interferons
72 (IFNs) (3), transforming growth factor-beta (TGF- β) (4), and interleukin-1-beta (IL-1 β) (5).
73 These restriction factors suppress viral replication by targeting the infection at various stages
74 of the virus life cycle, including viral entry (6), transcription of the viral genome (7), viral
75 RNA stability (8), translation of viral proteins (9), viral replication (10), and production of
76 viral particles (11).

77

78 Approximately 250 million people worldwide are chronically infected with Hepatitis B virus
79 (HBV). These patients are at high risk of developing life-threatening complications,
80 including hepatic cirrhosis, hepatic failure, and hepatocellular carcinoma. Current treatments
81 include nucleos(t)ide analogs that efficiently suppress HBV replication. However, an HBV
82 replication intermediate, covalently closed circular DNA (cccDNA), persists in the nucleus.
83 The cccDNA intermediate gives rise to progeny virus, and may lead to the development of
84 drug-resistant mutants and/or relapsing HBV after drug withdrawal (12). As such, new
85 strategies for HBV treatment are needed.

86

87 HBV has been identified in human remains from ~7000 years ago (13). This prolonged
88 history and evolution has shaped HBV to be one of the most successful of the “stealth”
89 viruses that can successfully establish infection while evading IFN induction (14). Although
90 HBV can evade IFN induction, the majority of HBV-infected adults (90%) are ultimately
91 able to clear the virus. This observation suggests that there are likely to be one or more IFN-
92 independent host restriction factors that facilitate HBV clearance.

93

94 The small Maf proteins (sMafs) are a family of basic-region leucine zipper (bZIP)-type
95 transcription factors. MafF, MafG and MafK are the three sMafs identified in vertebrate
96 species (15). Homodimers of these factors act as transcriptional repressors, consistent with
97 their lack of a transcriptional activation domain (16). Intriguingly, previous reports have
98 documented induction of MafF in myometrial cells by inflammatory cytokines, including IL-
99 1β and tumor necrosis factor alpha (TNF- α) (17). However, there have been no previous
100 studies that have addressed a role for MafF in promoting an anti-viral innate immune
101 response.

102 Epstein Bar Virus (EBV) is a human gamma herpesvirus that establishes primarily latent
103 infections in B lymphocytes. Only a small percentage of infected cells switch from the latent
104 stage into the lytic cycle and go on to produce progeny viruses (18). Although the mechanism
105 of EBV reactivation *in vivo* is not fully understood, it is known to be elicited *in vitro* by
106 treatment of latently infected B cells with chemical reagents, including 12-O-
107 tetradecanoylphorbol-13-acetate (TPA), calcium ionophores, or sodium butyrate. Treatment
108 with these reagents leads to the expression of two viral transcriptional regulatory genes, one
109 encoding BZLF1 (also known as ZEBRA) and the other encoding BRLF1, required for the
110 transition from the latent to the lytic productive stage of EBV [28].

111 Using an HBV reporter virus and an siRNA library, we performed functional siRNA
112 screening to identify the host factors that influence the HBV life cycle. Based on the results
113 of this screen, we identified MafF as a negative regulator of HBV infection. Further analysis
114 revealed that MafF functions as a repressor of transcription at the HBV core promoter,
115 thereby suppressing HBV replication. Interestingly, the antiviral effects of MafF also have
116 an impact on the life-cycle of EBV, as MafF negatively regulated the transcription of BZLF1
117 viral gene required for the reactivation of EBV from dormant to lytic (productive) stage. This
118 is the first study to report a role for MafF as an antiviral host factor that represses transcription
119 from the promoters of susceptible viruses.

120

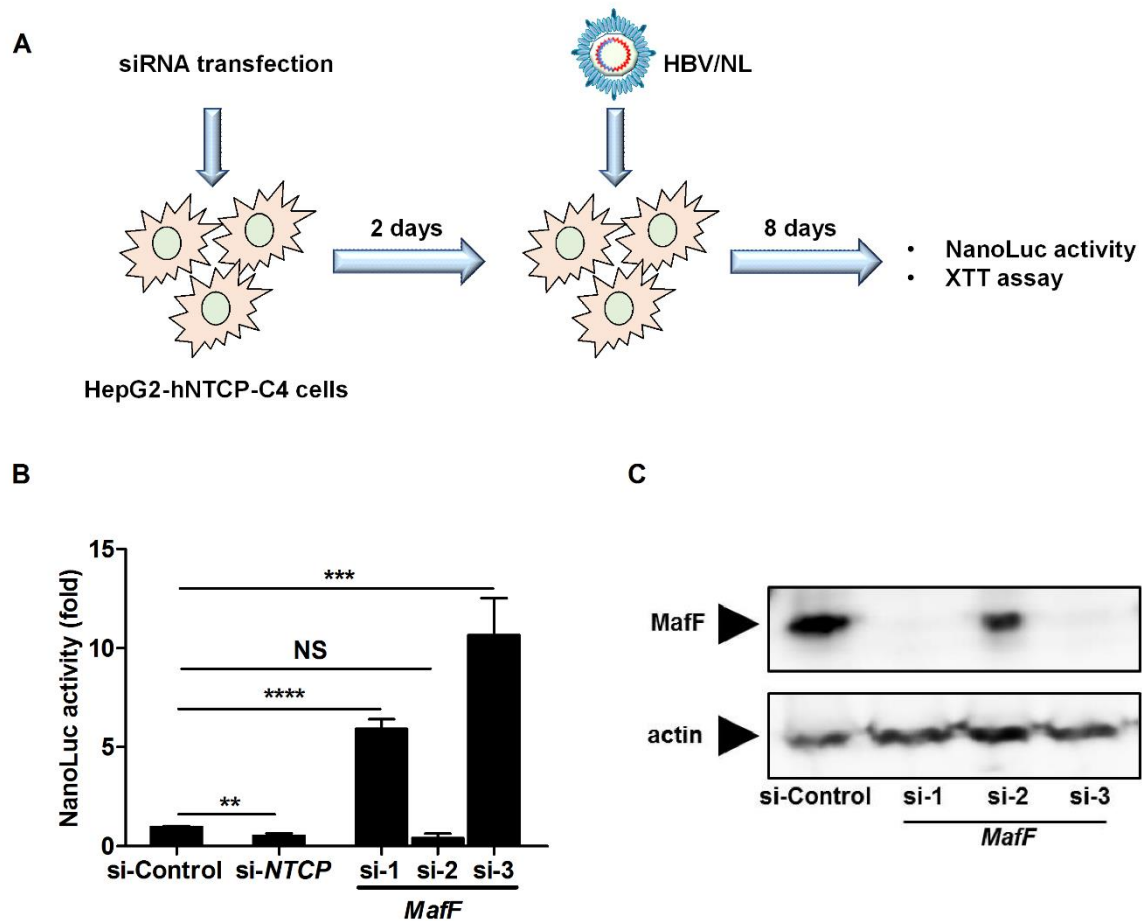
121

122

123 **Results**

124 **1. MafF suppresses expression of the HBV/NanoLuc (NL) reporter virus**

125 We screened for host factors that influence the HBV infection using the HBV/NL reporter
126 virus (19) in combination with the siRNA Library. This approach facilitated testing of 2200
127 human genes for their influence on the HBV life cycle. The screen was performed in HepG2-
128 C4 cells that express the HBV entry receptor, hNTCP (20). Non-targeting siRNAs, and
129 siRNAs against hNTCP, were used as controls for each plate (Fig. 1A). Cellular viability was
130 determined using the XTT assay; wells with $\geq 20\%$ loss of cell viability were excluded from
131 further evaluation. *MafF* was identified as an anti-HBV host factor based on independent
132 trials and silencing with at least two different siRNA sequences, both of which provided
133 greater than 2-fold induction of NanoLuc activity. Specifically, silencing of *MafF* expression
134 with si-1 or si-3 resulted in 6-fold ($p < 0.0001$) or 10-fold ($p < 0.001$) increases in NanoLuc
135 activity, respectively, compared to that observed in cells transfected with a control siRNA
136 (Fig. 1B). The MafF-specific sequence, si-2, did not show a similar effect (Fig. 1B). This
137 result was consistent with the fact that si-2 had a lower silencing efficiency with respect to
138 MafF expression (Fig. 1C). Taken together, these findings suggest that MafF may suppress
139 HBV infection.



140

141 **Figure 1. MafF suppresses HBV infection.**

142 **A.** A schematic diagram showing the experimental approach used to screen the siRNA library.

143 **B.** HepG2-hNTCP-C4 cells were transfected with control, *NTCP*, or *MafF*-targeting siRNAs

144 (si-1, si-2, and si-3); two days later, transfected cells were infected with the HBV/NL reporter

145 virus. At day 8 post-infection, luciferase assays were performed, and NanoLuc activity was

146 measured and plotted as fold-difference relative to the mean luciferase levels in control

147 siRNA-transfected cells. **C.** HepG2 cells were transfected with control or *MafF*-targeting

148 siRNAs (si-1, si-2, and si-3); total protein was extracted two days later. Expression of MafF

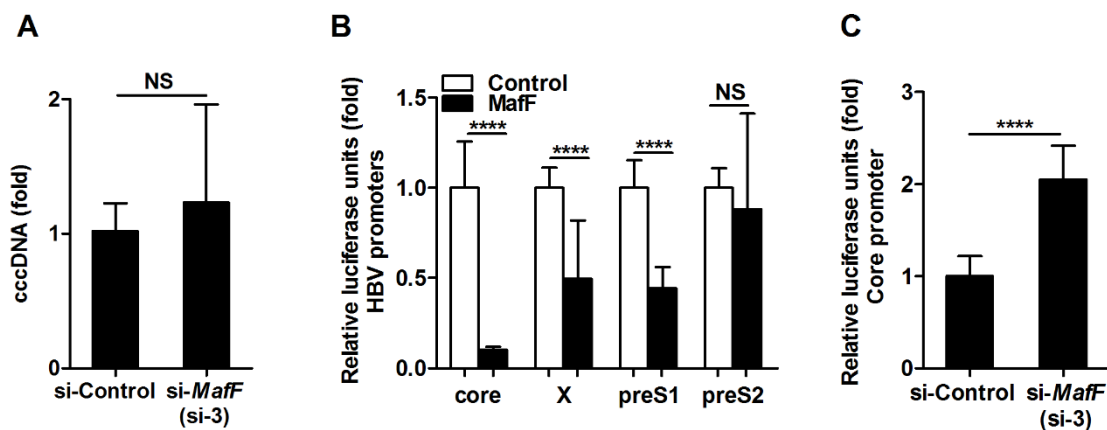
149 (upper panel) and actin (control; lower panel) was analyzed by immunoblotting with their

150 respective antibodies. All assays were performed in triplicate and included three independent

151 experiments; data are presented as mean±standard deviation (SD); ** $p < 0.01$, *** $p < 0.001$,
152 **** $p < 0.0001$; NS, not significant.

153 **2. MafF strongly suppresses HBV core promoter activity**

154 The HBV/NL reporter system can be used to detect factors affecting the early steps of the
155 HBV life cycle, from HBV entry through cccDNA formation, transcription and translation
156 of HBV pgRNA (19). Silencing of *MafF* had no impact on cccDNA levels observed in cells
157 infected with HBV (Fig. 2A); these results indicated that MafF suppressed the HBV life cycle
158 at stage that was later than that of cccDNA formation. Given that MafF can induce
159 transcriptional suppression (16), we analyzed the impact of MafF on various HBV promoters
160 (core, X, preS1, and preS2) using the HBV/NL luciferase reporter system. We found that
161 overexpression of MafF resulted in significant suppression of transcription from the HBV
162 core promoter (approximately 8-fold; $p < 0.0001$), and significant, albeit less of an impact on
163 transcription from the HBV-X and preS1 promoters (both at approximately 2-fold,
164 $p < 0.0001$); overexpression of MafF had no significant impact on transcription from the preS2
165 promoter (Fig. 2B). Likewise, siRNA silencing of endogenous *MafF* enhanced HBV core
166 promoter activity (Fig. 2C, $p < 0.0001$). Since the NanoLuc gene in HBV/NL virus (Fig. 1B)
167 is transcribed from an HBV core promoter (19), the findings presented in Fig. 1 and Fig. 2
168 collectively suggest that MafF-mediated suppression of HBV is mediated primarily by
169 inhibition of transcription from the core promoter.



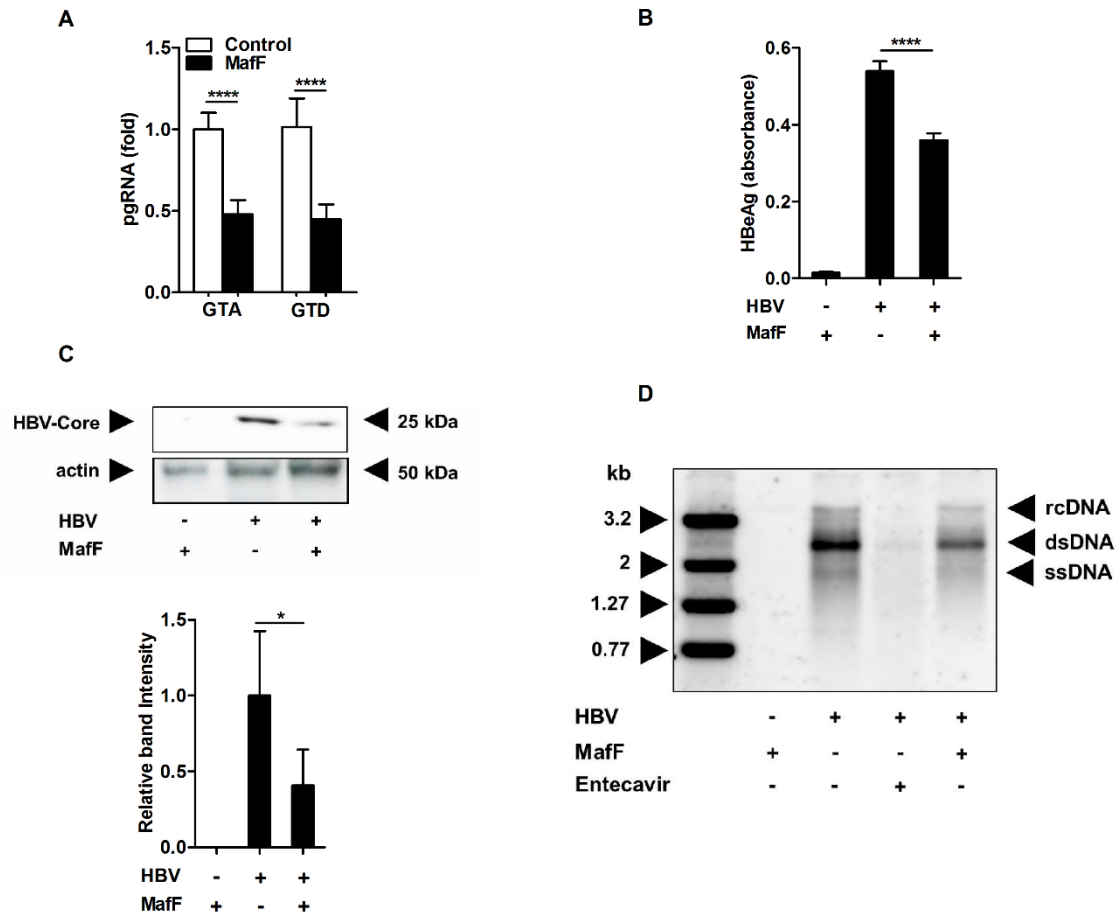
170

171 **Figure 2. MafF suppresses the transcriptional activity of the HBV core promoter.**

172 **A.** HepG2-hNTCP-C4 cells were transfected with control or *MafF*-targeting siRNA (si-3).
173 Two days after transfection, the transfected cells were infected with HBV at 12,000 genomic
174 equivalents (GEq) per cell. Eight days later, the cells were harvested, DNA was extracted,
175 and cccDNA was quantified by real-time PCR. The data were normalized to expression of
176 *GAPDH* and are presented as fold-change relative to control siRNA-transfected cells. **B.**
177 HepG2 cells were co-transfected with a *MafF* expression vector or empty vector (control)
178 together with firefly luciferase reporter plasmids with HBV promoters (core, X, S1, and S2)
179 and the pRL-TK control plasmid encoding *Renilla* luciferase. Two days after transfection,
180 the cells were harvested and evaluated by dual luciferase assay. **C.** HepG2 cells were
181 transfected with control or *MafF*-targeting siRNA (si-3); 24 hours later, the cells were
182 transfected with firefly luciferase reporter-HBV core promoter vector and the pRL-TK
183 plasmid encoding *Renilla* luciferase. Two days later, the cells were lysed and evaluated by
184 dual luciferase assay. For panels B and C, firefly luciferase data were normalized to *Renilla*
185 luciferase levels; relative light units (RLUs) for firefly luciferase were plotted as fold
186 differences relative to the levels detected in the control groups. All assays were performed in
187 triplicate and included three independent experiments; data are presented as mean \pm SD.
188 **** p <0.0001; NS, not significant.

189 **3. MafF suppresses HBV replication**

190 The HBV core promoter controls the transcription of the longest two HBV RNA transcripts,
191 the precore and pgRNAs. HBeAg is translated from the HBV precore RNA, while translation
192 of HBV pgRNA generates both the polymerase (Pol) and the capsid subunit; the pgRNA also
193 serves as the template for HBV-DNA reverse transcription (21, 22). As such, we assumed
194 that *MafF* served to inhibit HBV replication by controlling transcription of the HBV core
195 promoter. In fact, overexpression of *MafF* resulted in significant suppression of the pgRNA
196 titer of HBV genotypes A and D, as demonstrated by RT-qPCR (Fig. 3A, p <0.0001 for each
197 genotype). Overexpression of *MafF* also suppressed the release of HBeAg as measured by
198 ELISA (Fig. 3B, p <0.0001), as well as the intracellular accumulation of HBV core protein
199 as detected by immunoblotting (Fig. 3C upper and lower panels; p <0.05 by densitometric
200 analysis) and the level of HBV core-associated DNA as revealed by Southern blot (Fig. 3D).



201

202 **Figure 3. MafF suppresses HBV life cycle.**

203 **A.** HepG2 cells were transfected with empty (control) or MafF expression vector together
 204 with expression vectors encoding HBV genotypes A and D. Two days later, the cells were
 205 harvested and the pgRNA expression was quantified by real-time RT-PCR. The data were
 206 normalized to the expression of *GAPDH* and are shown as the fold-change relative to control
 207 plasmid-transfected cells. **B–D:** HepG2 cells were transfected with empty (control) or MafF
 208 expression vectors together with an expression plasmid encoding HBV genotype D (**B**) At 2
 209 days post-transfection, HBeAg in the cell culture supernatants were quantified by ELISA.
 210 (**C**) The intracellular levels of HBV core protein (upper left panel) and actin (loading control;
 211 lower left panel) were evaluated by immunoblotting; the intensities of the bands (right panel)
 212 were quantified by ImageJ software. (**D**) At 3 days post-transfection, the levels of

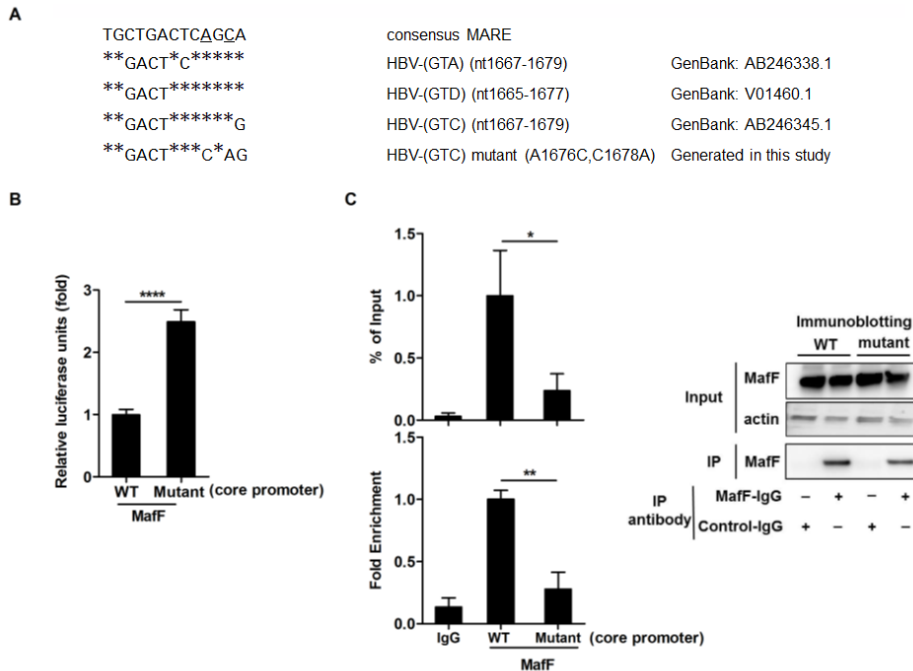
213 intracellular core-associated DNA were determined by Southern analysis; transfected cells
214 treated with 10 μ M entecavir were used as controls.

215 Data are presented as fold differences relative to the control plasmid-transfected cells. All
216 assays were performed in triplicate and include results from three independent experiments;
217 data are presented as mean \pm SD; * p <0.05, **** p <0.0001.

218 **4. MafF binds to the HBV core promoter**

219 We next analyzed the HBV core promoter for potential MafF binding sites using the JASPAR
220 database of transcription factor binding sites (23). Toward this end, we identified the
221 sequence 5'-TGGACTCTCAGCG-3' that corresponded to nucleotides (nts) 1667 to 1679 of
222 the HBV-C_JPNAT genome (GenBank AB246345.1) in the enhancer 2 (EnhII) of the HBV
223 core promoter. This motif was partially conserved among the various HBV genotypes (Fig.
224 4A) and was similar to a previously defined (16) Maf responsive element (MARE). The main
225 difference between this predicted MafF binding site and that of the endogenous Maf
226 recognition element (MARE; CTGA) was the sequence between the third and sixth
227 nucleotides which was replaced by a complementary (GACT) sequence in the HBV promoter
228 (Fig. 4A). As such, we evaluated the role of this predicted site with respect to HBV core
229 promoter activity. By analyzing JASPAR matrix (23) profile MA0495.1, we found that the
230 10th and 12th nucleotides of the aforementioned predicted MafF binding region, which are A
231 and C, respectively, are highly conserved residues. We disrupted the predicted HBV MARE
232 sequence by introducing 2-point mutations (A1676C and C1678A) into the HBV core
233 promoter. Interestingly, these mutations significantly counteracted the suppressive effect of
234 MafF at the HBV core promoter (Fig. 4B, p <0.0001). Furthermore, ChIP analysis revealed
235 that there was significantly less physical interaction between MafF and the HBV core
236 promoter with the double mutation than was observed between MafF and the HBV wild type
237 (WT) counterpart (Fig. 4C, p <0.05 for % of input and p <0.01 for fold enrichment). These
238 results confirmed that MafF physically binds to the WT HBV core promoter at the predicted
239 MafF binding site and thereby suppresses transcription. In its role as a transcriptional
240 repressor, MafF is known to homodimerize or to heterodimerize with other small Mafs
241 (MafG and MafK) that also lack transcriptional activation domains. We found that silencing

242 of *MafG* or *MafK* in the HepG2-C4 cells had no significant impact on HBV/NL infectivity
 243 (Supplementary Fig. 1A, B, and C). These data suggest that MafF most likely homodimerizes
 244 in order to suppress transcription from the HBV core promoter.



245
 246 **Figure 4. Physical interaction of MafF with HBV core promoter is required for**
 247 **transcriptional repression.**

248 **A.** A schematic representation of the putative MafF binding site (presented as a consensus
 249 Maf recognition element [MARE] sequence) within enhancer 2 (EnhII) of the HBV core
 250 promoter from the four different HBV genotypes. A mutant construct was prepared by
 251 introducing two point mutations (A1676C and C1678A) into the MARE sequence identified
 252 in the wild-type (WT) core promoter. * means consensus sequence, underlined nucleotides
 253 are HBV nucleotides 1676A and 1678C mutated in this study. **B.** HepG2 cells were co-
 254 transfected with a MafF expression plasmid along with an HBV core promoter (WT or
 255 mutant)-reporter plasmid and pRL-TK encoding *Renilla* luciferase. At two days post-
 256 transfection, a dual luciferase assay was performed; firefly luciferase data were normalized
 257 relative to *Renilla* luciferase levels, and RLU for firefly luciferase are plotted as fold
 258 differences relative to activity in the control group. **C.** 293FT cells were transfected with

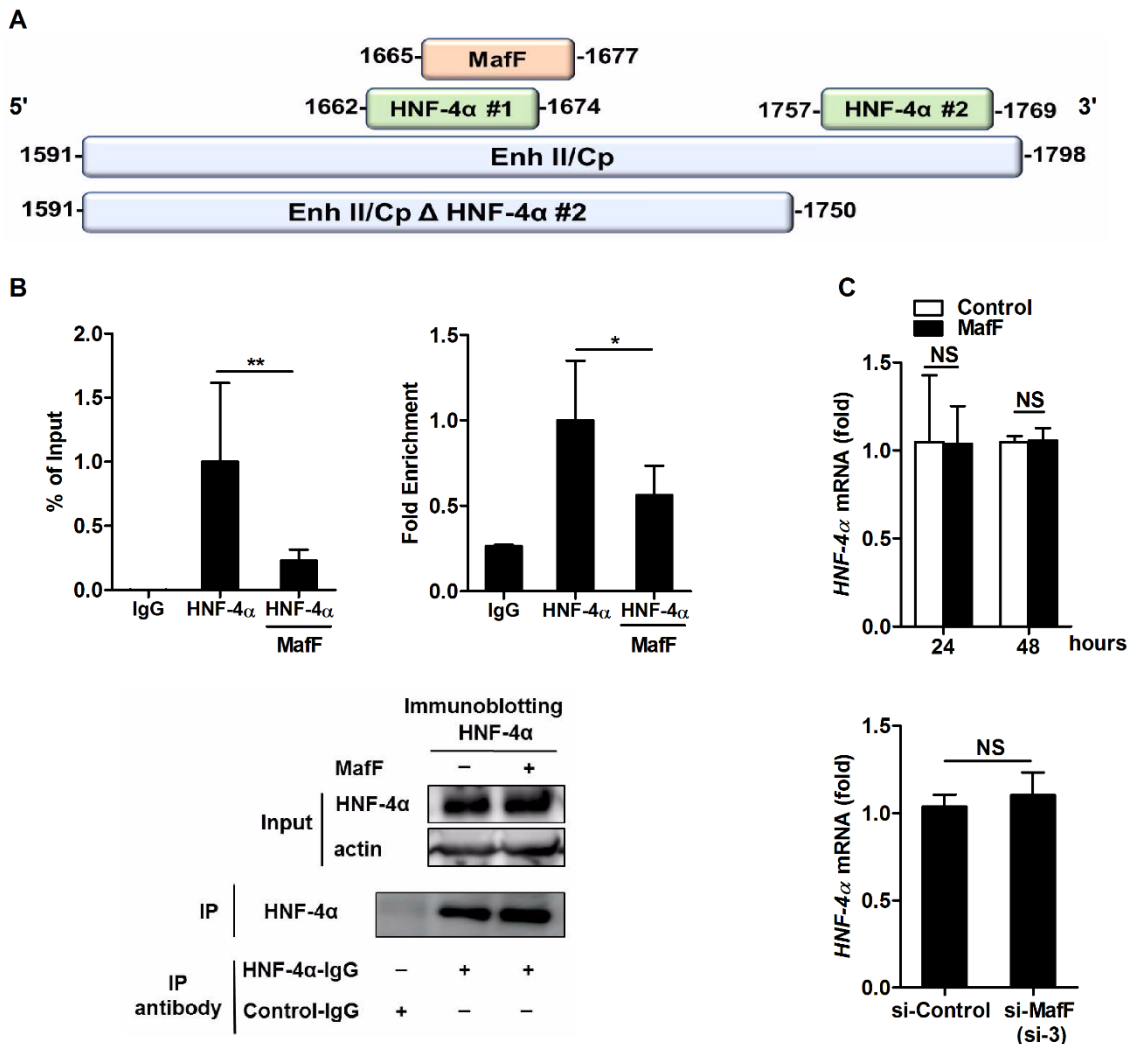
259 either the WT or mutant HBV core promoter-luciferase reporter plasmid together with a
260 MafF expression plasmid (at a ratio 1:4). At two days post-transfection, cell lysates were
261 collected; two aliquots (1/10 volume each) were removed from each sample. One aliquot was
262 used for the detection of MafF protein (Input) and actin (loading control) by immunoblotting
263 (upper and middle right panels); the second aliquot was used for DNA extraction and
264 detection of HBV core promoter (Input) by real-time PCR. The remaining cell lysates (each
265 8/10 of the original volume) were subjected to ChIP assay using either isotype control
266 antibody (rabbit IgG) or rabbit anti-MafF IgG to detect MafF. Following
267 immunoprecipitation (IP), 1/10 volume of each IP sample was analyzed by immunoblotting
268 for MafF (lower right panel); each remaining IP sample was subjected to DNA extraction
269 and real-time PCR assay in order to detect associated HBV core promoter DNA. The fraction
270 of core promoter DNA immunoprecipitated compared to the input value was determined by
271 real-time PCR and was expressed as percent of input (% of input) and as the fold enrichment
272 over the fraction of *GAPDH* DNA immunoprecipitated. The assays of panel B and C were
273 performed in triplicate and include data from three independent experiments. Data are
274 presented as mean±SD; * p <0.05, ** p <0.01, **** p <0.0001.

275

276 **5. MafF is a competitive inhibitor of hepatocyte nuclear factor (HNF)-4 α binding**
277 **to HBV EnhII**

278 HNF-4 α is a transcription factor that has been previously reported to bind HBV core
279 promoter and to induce its transcriptional activity (24-26). We found that the predicted MafF
280 binding site in the EnhII region overlaps with an HNF-4 α binding site that is located between
281 nucleotides 1662 to 1674 of the HBV C_JPNAT core promoter (27) (Fig. 5A). This finding
282 suggests the possibility that MafF may compete with HNF-4 α at these binding sites within
283 the EnhII region. To examine this possibility, we constructed a deletion mutant of EnhII/Cp
284 (EnhII/Cp Δ HNF-4 α #2) that extends from nt 1591 to nt 1750; this construct includes the
285 overlapping binding sites identified for MafF and HNF-4 α (i.e., HNF-4 α site #1 at nt 1662–
286 1674) but lacks the second HNF-4 α binding site (HNF-4 α site #2 at nt 1757–1769) as shown
287 in Fig. 5A. We performed a ChIP assay and found that the interaction between HNF-4 α and

288 EnhII/Cp Δ HNF-4 α #2 was significantly reduced in the presence of MafF (Fig. 5B, $p < 0.01$
 289 for % of input and $p < 0.05$ for fold enrichment). Furthermore, MafF had no impact on the
 290 expression of HNF-4 α (Fig. 5C). Together, these data indicated that MafF interacts directly
 291 with the HBV core promoter at the predicted binding site and suppresses the transcriptional
 292 activity of the HBV core promoter by competitive inhibition of HNF-4 α binding at an
 293 overlapping site in the EnhII region.



294

295 **Figure 5. MafF competes with HNF-4 α for binding to the HBV core promoter.**

296 **A.** A schematic representation of the enhancer 2 (EnhII) and the basal HBV core promoter
 297 (Cp; nt 1591-1798) featuring the MafF binding site (nt 1667–1679) and the two HNF-4 α

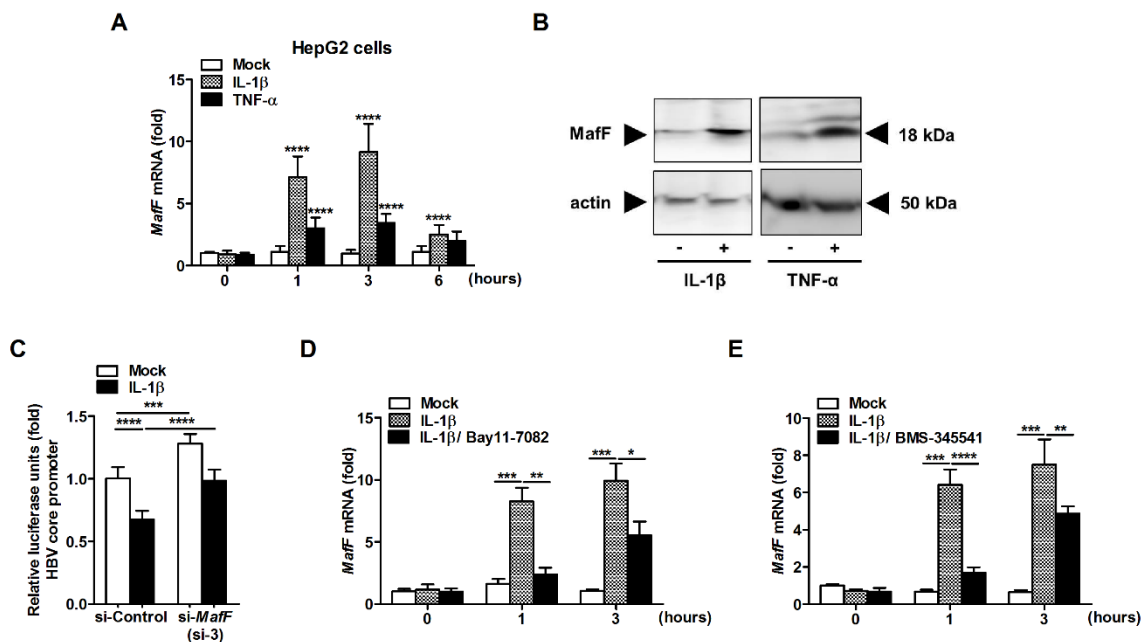
298 binding sites HNF-4 α #1 (nt 1662–1674) and HNF-4 α #2 (nt 1757–1769). A deletion mutant
299 construct (EnhII/Cp Δ HNF-4 α #2, nt 1591–1750) was prepared to eliminate HNF-4 α #2. **B.**
300 293FT cells were co-transfected with the EnhII/Cp Δ HNF-4 α #2-luciferase reporter plasmid,
301 a FLAG-tagged HNF-4 α expression plasmid, and a MafF (or control) expression plasmid at
302 a ratio of 1:1:2. At two days post-transfection, cell lysates were collected and two aliquots
303 (1/10 volume each) were removed from each sample. One aliquot was used for the detection
304 of HNF-4 α protein (Input) and actin (loading control) by immunoblotting (lower panel); the
305 second aliquot was used for DNA extraction and detection of HBV core promoter (Input) by
306 real-time PCR. The remaining cell lysates (each 4/10 of the original volume) were subjected
307 to ChIP assay using isotype control antibody (rabbit IgG) or rabbit anti-HNF-4 α IgG to
308 precipitate FLAG-tagged HNF-4 α . Following immunoprecipitation (IP), 1/5 volume of each
309 IP sample was analyzed by immunoblotting to detect HNF-4 α (lower panel) and each
310 remaining IP sample was subjected to DNA extraction and real-time PCR assay for the
311 detection of associated HBV core promoter DNA. The fraction of core promoter DNA
312 immunoprecipitated compared to the input value was determined by real-time PCR and was
313 expressed as percent of input (% of input) (upper left panel) and as the fold enrichment (upper
314 right panel) over the fraction of *GAPDH* DNA immunoprecipitated. **C. Upper panel:** HepG2
315 cells were transfected with empty vector (control) or MafF expression vector. After 24 h or
316 48 h, total RNA was extracted and *HNF-4 α* expression was quantified by real-time RT-PCR.
317 The data were normalized to *GAPDH* expression and are presented as fold differences
318 relative to the control cells. **Lower panel:** HepG2 cells were transfected with control or
319 *MafF*-targeting siRNA (si-3) and *HNF-4 α* expression was evaluated 48 h later as noted just
320 above. All assays were performed in triplicate and data are presented from three independent
321 experiments. Data are presented as mean \pm SD; * p <0.05, ** p <0.01; NS, not significant.

322

323 **6. IL-1 β and TNF- α -mediated induction of MafF expression *in vitro***

324 Given these findings, we speculated that MafF expression might be induced in hepatocytes
325 in response to HBV infection. Based on a previous report of the induction of MafF by both

326 IL-1 β and TNF- α in myometrial cells (17), and the fact that both of these cytokines have
 327 been implicated in promoting host defense against HBV, we explored the possibility that
 328 MafF might be induced by one or more of these cytokines in our *in vitro* system. As shown
 329 in Fig. 6, addition of IL-1 β or TNF- α resulted in significant induction of *MafF* mRNA
 330 expression in HepG2 cells (Fig. 6A, $p < 0.0001$ for each cytokine); MafF protein was also
 331 detected at higher levels in HepG2 cells exposed to each of these cytokines (Fig. 6B).
 332 Furthermore, IL-1 β suppressed HBV core promoter activity ($p < 0.0001$); silencing of *MafF*
 333 partially counteracted IL-1 β -mediated suppression ($p < 0.001$; Fig. 6C). Taken together, these
 334 data indicate that MafF contributes at least in part to the suppressive effects of IL-1 β on HBV
 335 infection via its capacity to suppress transcription from HBV core promoter.
 336 NF- κ B is a downstream regulatory factor that is shared by the IL-1 β and TNF- α signaling
 337 pathways. We found that chemical inhibition of NF- κ B activity with Bay11-7082 or BMS-
 338 3455415 suppressed the induction of *MafF* expression in response to IL-1 β (Fig. 6D and E;
 339 $p < 0.05$ for each of these inhibitors) and to TNF- α (Supplementary Fig. 2; $p < 0.01$). These
 340 findings indicate that the IL-1 β and TNF- α -mediated induction of *MafF* expression in
 341 hepatocytes is regulated by NF- κ B signaling.



342

343 **Figure 6. IL-1 β and TNF- α induce MafF expression via NF- κ B-mediated signaling.**

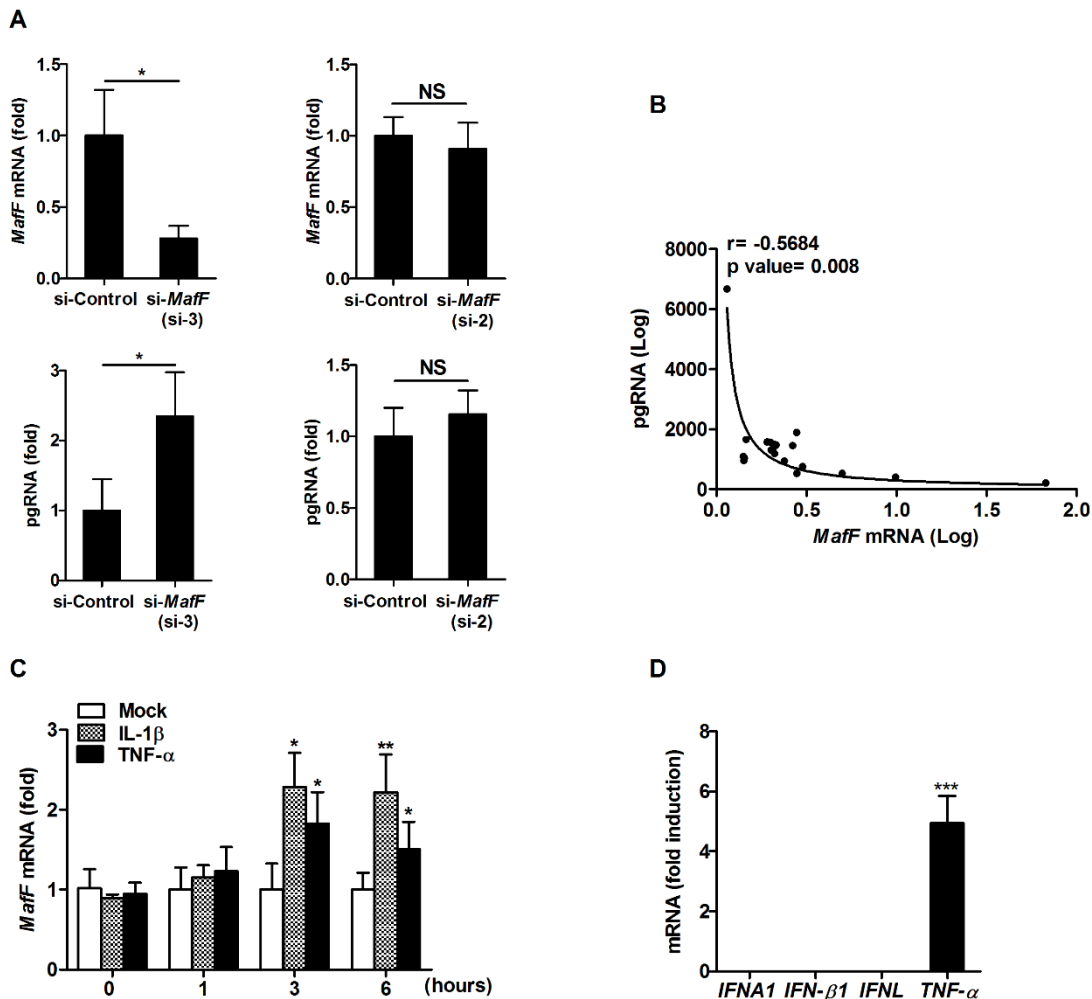
344 **A.** HepG2 cells were treated with IL-1 β (1 ng/ml), TNF- α (10 ng/ml), or PBS (diluent
345 control) for the times as indicated (hours). The cells then were lysed, total cellular RNA was
346 extracted, and *MafF* mRNA was quantified by real-time RT-PCR. The data were normalized
347 to the expression of *ACTB* and are shown as the fold-change relative to the mean of the
348 control group. **B.** HepG2 cells were treated for 24 h with IL-1 β , TNF- α , or PBS control as in
349 A.; the cells then were harvested and total protein was extracted. Expression of MafF (upper
350 panel) and actin (the loading control; lower panel) was analyzed by immunoblotting. **C.**
351 HepG2 cells were co-transfected with an HBV core promoter-reporter plasmid and the pRL-
352 TK plasmid (encoding *Renilla* luciferase) together with control or *MafF*-targeting siRNA (si-
353 3). At 2 days post-transfection, the cells were treated with 1 ng/ml IL-1 β or PBS (diluent
354 control) for 3 h; a luciferase assay was then performed. Data were normalized to the *Renilla*
355 luciferase activity, and the RLU were plotted as fold differences relative to the mean of the
356 luciferase activity of the PBS treated- control siRNA-transfected cells. **D–E.** HepG2 cells
357 were pre-treated with NF- κ B inhibitors Bay11-7082, BMS-345541, or DMSO (diluent
358 control) for 1 h and then treated with 1 ng/ml IL-1 β or PBS (control) for 1 and 3 h. Expression
359 of MafF was quantified as described in A. All assays were performed in triplicate and
360 including the results from three (panels A, B, and C) or two (E and F) independent
361 experiments. Data are presented as mean \pm SD; * p <0.05, ** p <0.01, *** p <0.001, **** p <
362 0.0001.

363

364 **7. MafF targets HBV infection in human primary hepatocytes**

365 To confirm the suppressive effects of MafF on HBV infection in a more physiological context,
366 we silenced *MafF* expression in human primary hepatocytes (PXB cells) using two
367 independent siRNAs, including si-3 which efficiently targets the *MafF* transcript, and si-2
368 which was associated with a negligible silencing efficiency (Fig. 1C and Fig. 7A, upper
369 panels), followed by infection with HBV (genotype D). *MafF* silencing in response to si-3
370 resulted in significant induction of HBV-pgRNA (Fig. 7A, lower panels; p <0.05);
371 administration of si-2 did not yield a similar effect. In all experiments, transcription of

372 pgRNA was inversely associated with expression of *MafF* (Fig. 7B, $p=0.008$); these findings
 373 confirmed the role of endogenous *MafF* with respect to the regulation of HBV-pgRNA
 374 transcription. To confirm our earlier findings documenting induction of *MafF* by IL-1 β and
 375 TNF- α , we treated PXB cells with both cytokines and observed a significant increase in *MafF*
 376 mRNA (Fig. 7C, $p<0.05$ for each cytokine).



377

378 **Figure 7. MafF suppresses HBV infection in primary human hepatocytes (PXB cells).**

379 **A.** Primary hepatocytes (PXB cells) were infected with HBV virions at 5,000 GEq per cell.
 380 After 3 days, the cells were transfected with control or *MafF*-targeting siRNAs (si-2 and si-
 381 3); at 4 days after transfection, total RNA was extracted. **Upper panel:** *MafF* expression
 382 level was quantified by real-time RT-PCR and normalized to the expression of *ACTB*. **Lower**

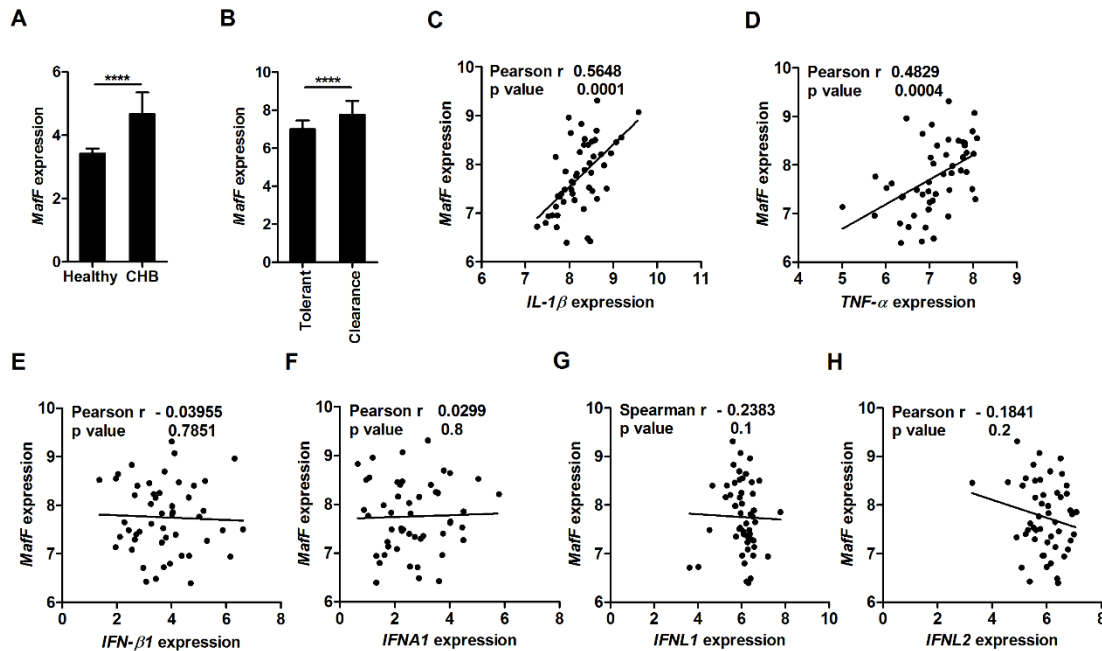
383 **panel:** Levels of pgRNA were quantified by real time RT-PCR using a standard curve
384 quantification method. Data are presented as fold differences relative to the control siRNA-
385 transfected cells. **B.** Correlation between expression of *MafF* mRNA and pgRNA in HBV-
386 infected and siRNA transfected PXB cells as described in A. **C.** Primary hepatocytes (PXB)
387 cells were treated with IL-1 β (at 10 ng/ml), TNF- α (at 10 ng/ml), or PBS (diluent control) for
388 the times indicated (hours). The cells then were lysed, total cellular RNA was extracted, and
389 *MafF* mRNA was quantified by real-time RT-PCR. The data were normalized to the
390 expression of *ACTB* and are shown as the fold change relative to the mean of the control
391 group. All assays were performed in triplicate and include data from two independent
392 experiments. Data are presented as mean \pm SD; * p <0.05, ** p <0.01; NS, not significant.

393

394 **8. *MafF* expression is higher in HBV chronically infected patients with a positive**
395 **correlation to *IL-1 β* and *TNF- α* expression**

396 To explore a role for MafF in HBV infection in human subjects, we evaluated data from an
397 open database (28), and found that *MafF* was expressed at significantly higher levels in
398 patients with chronic HBV compared to healthy individuals (Fig. 8A, p <0.0001); this was
399 notably the case in patients undergoing immune clearance HBV (Fig. 8B, p <0.0001). This
400 result confirmed the induction of *MafF* expression during active inflammation associated
401 with this infection. This observation was strengthened by the demonstration of positive
402 correlations between the levels of *IL-1 β* and *TNF- α* transcripts and those encoding *MafF* in
403 the immune clearance patient subset (Fig. 8C, D). Interestingly, no correlations were
404 observed between *MafF* expression and transcripts encoding IFNs (Fig. 8E, F, G, and H).
405 These data suggest that MafF induction associated with chronic HBV disease was unrelated
406 to induction of IFN signaling pathways.

407



408

409 **Figure 8. *MafF* expression is increased in patients with chronic HBV infections and is**
 410 **positively correlated to expression of *IL-1β* and *TNF-α* mRNAs**

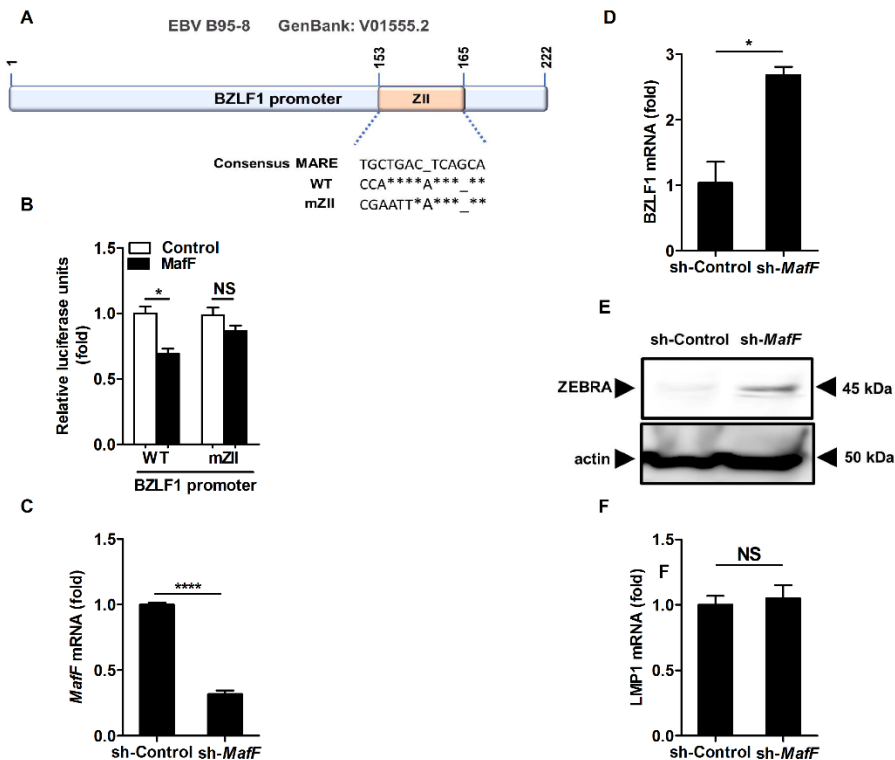
411 **A.** *MafF* mRNA levels in the liver tissue of patients with chronic hepatitis B infection (CHB;
 412 n=122) and healthy subjects (n=6, GSE83148). **B.** *MafF* mRNA levels in the liver tissue of
 413 immune-tolerant (n=22) and immune-clearance (n=50) HBV-infected patients (GSE65359).
 414 **C.-H.** Correlations between the expression of mRNAs encoding *MafF* and **C.** *IL-1β*, **D.** *TNF-*
 415 *α*, **E.** *IFN-β1*, **F.** *IFNA1*, **G.** *IFNL1*, and **H.** *IFNL2* in liver tissue of patients undergoing
 416 immune-clearance. In panels A and D, data are presented as the mean±SD; *****p*<0.0001.

417

418 **9. MafF suppresses expression of BZLF1, a key player for switching from the**
 419 **latency to the lytic phase of EBV infection.**

420 To determine whether MafF-mediated restriction is limited to HBV or has broader antiviral
 421 effects, we explored the impact of MafF on another DNA virus, Epstein Barr virus (EBV).
 422 BZLF1 (ZEBRA) is a transcriptional activator with structural features of other members of
 423 the basic leucine zipper (b-Zip) family. BZLF1 expression triggered the reactivation of EBV
 424 from the latent to the lytic (productive) stage (29). In addition, it also activates transcription

425 from its own promoter (30). Previous reports indicated that ZII, positive regulatory element,
 426 in BZLF1 promoter is a binding site for AP1, CREB/ATF, and MafB b-Zip transcriptional
 427 activators (31). Since MARE is known to occur in close association with these transcription
 428 factors binding sites (32), we speculated that MafF may bind to and suppress transcription
 429 from BZLF1 promoter via ZII. A comparison between the MARE consensus sequence and
 430 ZII sequence is shown in Fig. 9A. In fact, we found that MafF suppressed transcription from
 431 the BZLF1 promoter; which was not observed when mutant BZLF1 promoter (mZII) in
 432 which b-Zip binding site is mutated, was used ((31); Fig. 9B, $p < 0.05$). Similarly, stable
 433 silencing of MafF in Raji cells, an EBV-positive B cell line, using *MafF* shRNA (Fig. 9C)
 434 alone, without the use of chemical inducers such as 12-O-tetradecanoylphorbol-13-acetate
 435 (TPA), led to an increase in BZLF1 mRNA (Fig. 9D, $p < 0.05$) and protein (ZEBRA protein,
 436 Fig. 9E). By contrast, MafF silencing had no impact on the latency stage gene, LMP1 (Fig.
 437 9F). Overall, these data indicate that endogenous MafF may suppress reactivation of EBV
 438 lytic phase and the resulting EBV proliferation by the repression of BZLF1 transcription.



439

440 **Figure 9. MafF suppresses expression of BZLF1, a key player of switch from latency to**
441 **lytic phase**

442 **A.** A schematic representation of the BZLF1 promoter of EBV B95-8 (nt 1-222), and a
443 comparison between the MARE consensus sequence and b-Zip binding site (ZII) sequence
444 of the wild type (WT) promoter and mutated (mZII) promoter. * and under bar (_) represent
445 identical sequence and deletion, respectively. **B.** 293 FT cells were co-transfected with a
446 MafF expression plasmid together with EBV BZLF1 promoter constructs, including WT
447 (pzp-luc) and b-Zip binding site mutated (pzp-luc mZII)-reporter plasmids and pRL-TK
448 which encodes *Renilla* luciferase. At two days post-transfection, a dual luciferase assay was
449 performed; firefly luciferase data were normalized relative to *Renilla* luciferase levels; RLU
450 for firefly luciferase are plotted as fold differences relative to activity in the control group.
451 **C-F.** Raji cells were stably transfected with control or *MafF*-targeting shRNA and selected
452 with puromycin (2 µg/ml) for 10 days. **C, D, and F.** Total RNA was extracted and expression
453 of *MafF*, BZLF1, and LMP1 was quantified by real-time RT-PCR. The data were normalized
454 to the expression of the housekeeping gene *GAPDH*, and are presented as fold differences
455 relative to the control cells. **E.** The expression of both ZEBRA (upper panel) and actin (the
456 loading control; lower panel) were evaluated by immunoblotting. All assays were performed
457 in triplicate and include data from three independent experiments. Data are presented as
458 mean±SD; * $p<0.05$, **** $p<0.0001$; NS, not significant.

459

460 **Discussion**

461 The intrinsic, or innate immune response is mediated by cellular restriction factors.
462 Many of these factors induced by cytokines (3-5) and serve to suppress different stages of
463 the viral life cycle, from entry to virion release (2). Several host restriction factors can
464 suppress transcription from DNA virus promoters (7, 33). In this work, we identified MafF
465 as a new host restriction factor that can inhibit both HBV and EBV infections via
466 transcriptional suppression at targeted viral promoters.

467 MafF is a member of the small Maf (sMaf) family of transcription factors, a group
468 that includes MafG (34), MafK, and MafF (35). The sMafs are bZIP-type transcription

469 factors that bind to DNA at Maf recognition elements (MAREs). MAREs were initially
470 defined as a 13-bp (TGCTGA(G/C)TCAGCA) or 14-bp (TGCTGA(GC/CG)TCAGCA)
471 elements (36, 37). However, multiple studies (38-40) have presented findings suggesting
472 heterogeneity within MARE sequences. Using the JASPAR database for transcription factor
473 binding sites, we identified a sequence extending from nt 1667 to 1679
474 (TGGACTCTCAGCG) in the EnhII region of HBV as a potential MafF binding site. Both
475 ChIP and functional analysis confirmed the importance of the interaction between MafF and
476 this specific sequence in HBV core promoter; MafF binding at this site results in suppression
477 of the transcriptional activity from HBV core promoter and inhibition of the HBV life cycle.
478 Interestingly, the MafF binding site in the HBV core promoter was conserved among the
479 multiple HBV genotypes; MafF-mediated suppression was also observed more broadly at
480 core promoters from HBV genotypes A, C, and D.

481 The expression levels of sMafs serve as strong determinants of their overall function.
482 An excess of sMafs may increase the level of homodimer formation and shift the balance
483 toward transcriptional repression (41). Of note, sMafs can form homodimers or serve as
484 partners for heterodimer formation with cap'n'collar (CNC) family proteins Nrf1, Nrf2, Nrf3,
485 Bach1, and Bach2 (42). Furthermore, MARE consensus sites include an embedded canonical
486 AP1 motif; as such, some Jun and Fos family factors can also heterodimerize with Maf/CNC
487 proteins. Finally, large Maf proteins are also capable of binding at MARE elements (43, 44).
488 Given the large number of possible homo- and heterodimeric combinations of proteins
489 capable of binding to MAREs, transcriptional responses ranging from subtle to robust can be
490 elicited at a single MARE site (44). The inflammatory response to virus infection facilitates
491 the production of cytokine-inducible host factors that can repress transcription from factors
492 binding at MAREs; these factors serve to suppress replication of DNA viruses that depend
493 on the aforementioned network for the transcriptional activation at its promoters. Of note,
494 our findings revealed that MafF expression is induced by IL-1 β and TNF- α in primary
495 hepatocytes (PXBs) and that this induction was mediated by NF- κ B, an inducible
496 transcription factor that is a central regulator of immune and inflammatory responses (45).
497 Both IL-1 β and TNF- α have been associated with protection against HBV. For example, a

498 polymorphism in the IL-1 β -gene has been linked to disease progression in patients with
499 HBV-related hepatitis (46), while TNF- α expression in hepatocytes induced by HBV (47)
500 has been shown to decrease the extent of HBV persistence (48). We detected higher levels of
501 *MafF* expression in patients with chronic HBV, especially among those in the immune
502 clearance group, compared to healthy individuals. Moreover, we have also reported that
503 silencing of *MafF* expression resulted in partial rescue of IL-1 β -mediated suppression of
504 transcription from the HBV core promoter. Taken together, these data suggest an important
505 role for MafF with respect to the anti-HBV effects of these cytokines in HBV-infected
506 patients.

507 Transcription driven from HBV core promoter is controlled by two enhancers,
508 enhancer I (EnhI) and EnhII, the latter overlapping with the core promoter (EnhII/Cp);
509 transcription is also modulated by a negative regulatory element (NRE) (49). Liver-enriched
510 transcription factors, including C/EBP α , HNF-4 α , HNF3, FTF/LRH-1, and HLF4, can
511 interact with the EnhII/Cp region and thereby enhance the core promoter activity (50, 51).
512 Negative regulation of HBV core promoter mainly takes place at the NRE, which is located
513 immediately upstream of EnhII (52). Our analysis of the EnhII segment revealed an overlap
514 between MafF and one of the HNF-4 α binding sites located between nt 1662 to nt 1674. We
515 identified MafF as a novel negative regulator of EnhII activity that acts via competitive
516 inhibition of HNF-4 α binding to the HBV core promoter at this site; we present this
517 mechanism as a plausible explanation for MafF-mediated suppression of HBV infection.

518 MafF mediated significantly stronger suppression of transcription from HBV core
519 promoter compared to its actions at HBV-X and PreS1; this is likely due to the
520 aforementioned direct interaction between MafF and core promoter. MafF may not be
521 involved in direct interactions with HBV-X and PreS1 promoters, but may play a role via
522 interactions with other transcription factors that regulate transcription from these promoters.
523 HBV core promoter regulates the expression of HBV-precure and pgRNA transcripts. The
524 precure-RNA serves as the template for the translation of HBV-precure protein. HBV-
525 pgRNA is translated into two proteins, HBc (the capsid-forming protein) and pol
526 (polymerase); the HBV-pgRNA also serves as a template for HBV-DNA reverse

527 transcription and viral replication (53). MafF inhibits HBV replication via suppressing the
528 production of HBV-pgRNA, thereby limiting the production of the corresponding
529 replication-associated proteins (core and pol; Fig. 3). We showed here that HBV-pgRNA
530 titers in HBV-infected primary hepatocytes (PXB) were higher in cells subjected to MafF
531 silencing; levels of HBV-pgRNA were inversely correlated with MafF mRNA levels (Fig.
532 7A and B). These data confirmed the importance of endogenous MafF with respect to the
533 regulation of HBV-pgRNA transcription and viral replication. The HBV precore protein is a
534 well-known suppressor of the anti-HBV immune response (54-56). As such, suppression of
535 HBV precore protein expression may promote a MafF-mediated recovery of the anti-HBV
536 immune response and enhanced viral clearance.

537 We found here that silencing of MafF expression induced the transcription of BZLF1,
538 resulting in increases in BZLF1 mRNA, and ZEBRA protein levels. These data suggest that
539 MafF may have a strong role in preventing of EBV reactivation through suppression of
540 BZLF1 expression. We described the induction of MafF expression by IL-1 β and TNF- α
541 inflammatory cytokines through NF- κ B signaling in human hepatocytes. Interestingly, both
542 TNF- α and NF- κ b signaling were previously reported to promote EBV latency by negatively
543 regulating BZLF1 transcriptional activity (57). Knowing that MafF expression was induced
544 by the TNF- α in NF- κ B dependent manner (Fig. 6), pauses MafF as a possible inducer for
545 the suppression of BZLF1 transcriptional activity reported by this signaling pathway.

546 To summarize, the results of this work identified MafF as a novel anti-HBV and anti-
547 EBV host factor. *MafF* expression was induced by both IL-1 β and TNF- α in primary
548 hepatocytes and also in patients with chronic HBV. Furthermore, MafF was shown to play
549 an important role in the suppression of transcription from the HBV core promoter as well as
550 the EBV BZLF1 promoter. Further analysis will be needed in order to determine whether the
551 anti-viral function of MafF is effective against other DNA viruses as well as its impact on
552 viral evasion mechanisms.

553

554

555 **Materials and Methods**

556 **Cell culture**

557 All the cells used in this study were maintained in culture at 37°C and 5% CO₂. HepG2,
558 HepG2-hNTCP-C4, and HepAD38.7-Tet cell lines were cultured in Dulbecco's modified
559 Eagle's medium/F-12 (DMEM/F-12) GlutaMAX media (Gibco) as previously described (20).
560 Primary human hepatocytes (Phoenixbio; PXB cells) were cultured as previously described
561 (58). HEK 293FT cells were cultured in DMEM (Sigma), and Raji Burkitt's lymphoma cells
562 were cultured in Roswell Park Memorial Institute media (Gibco) as previously described (8,
563 59).

564

565 **siRNA library**

566 A Silencer Select™ Human Druggable Genome siRNA Library V4 was used for screening
567 of HepG2-hNTCP-C4 cells infected with the HBV/NL reporter virus. The siRNAs were
568 arrayed in a 96-well format; siRNAs targeting the same genes with different target sequences
569 were distributed across three plates (A, B, and C). The following plates from this siRNA
570 library (2200 human genes) were screened: 1-1, 1-2, 1-3, 1-4, 2-1, 2-2, 2-3, 2-4, 3-1, 5-4, 6-
571 2, 6-3, 9-2, 11-3, 11-4, 13-3, 15-1, 15-4, 19-1, 22-2, 25-3, 25-4, 26-1, 26-2, and 26-3. Cellular
572 viability was determined using the XTT assay (Roche) according to the manufacturer's
573 instructions. Wells with $\geq 20\%$ loss of cell viability were excluded from further evaluation.
574 Protocols for the preparation of HBV/NL and screening were as described previously (19).

575 **Plasmid vectors**

576 An HBV genotype D subtype ayw replicon (60) was obtained from Addgene. HBV Ae
577 (genotype A), HBV D_IND60, and HBV C_JPNAT are 1.24 HBV replicons which were
578 described previously (61). A MafF expression plasmid (pFN21AB8874) was purchased from
579 Promega. To add a C-terminal HaloTag, the MafF-encoding sequence was subcloned into
580 the PC14K HaloTag vector using the Carboxy Flexi system (Promega). Additional details
581 regarding the construction of other plasmids are included in the Supplementary Materials.

582 **DNA and RNA transfection**

583 Plasmid DNA transfection was performed according to the manufacturer's guidelines, using
584 Lipofectamine 3000 (Invitrogen) for HepG2 cells and Lipofectamine 2000 (Invitrogen) for
585 HEK 293FT cells. Reverse siRNA transfection into HepG2-hNTCP-C4 was performed using
586 Lipofectamine RNAiMAX (Thermo Fisher Scientific); forward siRNA transfection was
587 performed in PXB cells only using Lipofectamine RNAiMAX or in HepG2 using
588 Lipofectamine 2000 for siRNA/DNA co-transfection studies according to the respective
589 manufacturer's guidelines. Silencer Select™ si-*MafF* (s-1, s24372; s-2, s24371; and s-3,
590 s24370), si-*MafK* (s194858), si-*MafG* (s8419), and the negative control siRNA (#2) were
591 purchased from Thermo Fisher Scientific.

592 **Western blot analysis**

593 Cells were lysed with PRO-PREP protein extraction solution (Intron Biotechnology). Protein
594 samples were separated on a 12% gel via SDS-PAGE. Immunoblotting and protein detection
595 were performed as previously reported (8). Primary antibodies included mouse monoclonal
596 anti-HBc (provided by Dr. Akihide Ryo, Yokohama City University), anti-Halo-tag
597 (Promega), anti-FLAG (M2, Sigma), Anti-EBV ZEBRA (BZ1 IgG, Santa Cruz), and anti-
598 actin (Sigma), rabbit polyclonal anti-MafF (Protein Tech), and rabbit monoclonal anti-HNF-
599 4 α (Abcam). The band intensities were quantified by ImageJ software (NIH).

600 **HBV preparation and infection**

601 HBV and HBV/NL stocks used in this study were prepared as described previously (19, 20)
602 For infection of HepG2-hNTCP-C4 cells, the cells first were reverse-transfected with *MafF*
603 or negative control siRNAs two days prior to the HBV infection, and then infected 2 days
604 later with inoculation of HBV or HBV/NL as described previously (19, 20); the experiment
605 was terminated at 8 days post-infection. For PXB cells, the cells were first infected with
606 HBV; at 3 days post-infection, the cells were transfected with the siRNAs, and the experiment
607 was terminated at 7 days post-infection.

608 **RNA extraction and quantitative real-time PCR**

609 Isolation of total cellular RNA was performed with a RNeasy Mini kit (Qiagen) according to
610 the manufacturer's guidelines and cDNA synthesis was performed using a Superscript VILO

611 cDNA Synthesis Kit (Thermo Fisher Scientific). Primer and probe sequences are included in
612 the Supplementary materials.

613 **DNA extraction and cccDNA quantification**

614 For selective extraction of cccDNAs, HBV-infected HepG2-hNTCP-C4 cells were harvested
615 and total DNA was extracted using a Qiagen DNA extraction kit according to the
616 manufacturer's instructions but without the addition of Proteinase K as recommended by the
617 concerted harmonization efforts for HBV cccDNA quantification reported in the 2019
618 International HBV meeting (62). Levels of cccDNA were measured by quantitative real-time
619 PCR (qPCR) using the TaqMan Gene Expression Master Mix (Applied Biosystems), specific
620 primers, and probe as described previously (63). Data were processed as $2^{(-\Delta\Delta C_t)}$ for
621 quantification of cccDNA using *GAPDH* (via primer-probe set Hs04420697_g1; Applied
622 Biosystems) as an internal normalization control.

623 **Dual luciferase reporter assay**

624 Firefly luciferase reporter plasmids carrying the entire HBV core promoter (nt 900 to 1817),
625 the Enh1/X promoter (nt 950 to 1373), the preS1 promoter (nt 2707 to 2847), or the preS2/S
626 promoter (nt 2937 to 3204) were constructed as previously reported (64). The WT (pzp-luc)
627 and mutated BZLF1 (pzp-luc mZII) luciferase reporter plasmids were also as previously
628 reported (65). HepG2 or 293FT cells were co-transfected with the firefly reporter vectors and
629 the *Renilla* luciferase plasmid pRL-TK (Promega) as an internal control. At 48 h post-
630 transfection, the cells were lysed and luciferase activities were measured using the Dual-
631 Luciferase Reporter Assay System (Promega). For experiments involving IL-1 β , cells were
632 treated for 3 h with IL-1 β (1 ng/ml) at 48 h post-transfection followed by evaluation of dual
633 luciferase activity.

634 **Quantification of HBe antigen**

635 Cell supernatants were harvested and an enzyme-linked immunosorbent assay (ELISA;
636 Enzygnost HBe monoclonal, Siemens) was used to determine the levels of HBe antigen in
637 the culture supernatants according to the manufacturer's instructions.

638 **Southern blotting assay**

639 HepG2 cells were co-transfected with MafF-encoding or control vectors together with the
640 HBV ayw plasmid both with or without 5 μ M entecavir (Sigma) as a control. At 3 days post-
641 transfection, core-associated DNA was isolated from intracellular viral capsids as described
642 previously (66). Southern blot analysis to detect HBV-DNAs was performed also as
643 described previously (8)

644 **Chromatin Immunoprecipitation (ChIP) assay**

645 293FT cells were co-transfected with a MafF expression plasmid together a reporter plasmid
646 harboring either the wild-type (WT) or mutated core promoter (substitution mutations in
647 MARE) at a 4:1 ratio for assessment of the interactions between MafF and HBV core
648 promoter. In other experiments, 293FT cells were co-transfected with plasmids encoding
649 FLAG-tagged HNF-4 α , EnhII/CP Δ HNF-4 α #2, and a MafF expression plasmid (or empty
650 vector) at a 1:1:2 ratio for assessment of competitive binding of MafF and HNF-4 α . At 48 h
651 post-transfection, ChIP was carried out using a Magna ChIP G kit (Millipore) according to
652 the manufacturer's instructions. Additional detailed information is included in the
653 Supplementary materials.

654 **Cytokine treatment and NF- κ B inhibitors**

655 Responses to IL-1 β and TNF- α (R&D Systems) were evaluated in HepG2 cells (at 1 ng/ml
656 and 10 ng/ml, respectively) and in PXB cells (both at 10 ng/ml) after 1, 3, and 6 h. For the
657 experiments involving NF- κ B inhibitors, Bay11-7082 and BMS-345541 (both from Tocris)
658 were added to final concentrations of 10 μ M and 5 μ M, respectively. HepG2 cells were pre-
659 treated for 1 h with each inhibitor followed by the addition of 1 ng/ml IL-1 β (for 1 and 3 h)
660 or 10 ng/ml TNF- α (for 1 h). All experiments included phosphate-buffered saline (PBS) as a
661 diluent control for the cytokines and dimethyl sulfoxide (DMSO) as the diluent control for
662 the NF- κ B inhibitors.

663 **Database**

664 Transcriptional profiling of the patients with chronic HBV (CHB) (GSE83148), and of HBV
665 patients with immune-tolerance and undergoing HBV clearance (GSE65359) were identified
666 in the Gene Expression Omnibus public database. Expression data for *MafF* and for genes

667 encoding cytokines *IL-1 β* , *TNF- α* , *IFNA1*, *IFN- β 1*, *IFNL1*, and *IFNL2* were extracted by
668 GEO2R.

669 **Construction and stable transfection with shRNA.**

670 The pLKO.1-puro lentivirus expression vector was digested with *AegI* and *EcoRI* and
671 annealed with oligonucleotides including sh-MafF: 5'-
672 aggacgaggtaccggtaGCCTTTTGTAGATTGAGAGATTctcgagAATCTCTCAATCTAAAA
673 GGctattttgaattctagatcttga-3' or sh-control (67) that were ligated into the vector. For the
674 production of lentivirus vectors, 293FT cells were transfected with expression plasmids
675 encoding HIV-1 Gag-Pol, and VSV G, and shRNAs (sh-control, and sh-MAfF) using
676 Lipofectamine 2000 (Invitrogen). Culture supernatants were collected at t = 60 hours. Raji
677 cells were infected with the lentiviral constructs in the presence of 10 μ g/mL Polybrene. Bulk
678 selection of cells in with stable integration of the shRNA construct was performed by the
679 addition of Puromycin (2 μ g/mL) to the culture supernatant.

680 **Statistical analysis**

681 The data were analyzed with algorithms included in Prism (v. 5.01; GraphPad Software, San
682 Diego, CA). Tests for normal distribution of the data were performed. Two-tailed unpaired t
683 tests, and Mann-Whitney U tests were used for statistical analysis of parametric and non-
684 parametric data, respectively. The correlation coefficients were determined by Pearson or
685 Spearman correlation analysis of parametric and non-parametric data, respectively. Values
686 of $p \leq 0.05$ were considered statistically significant.

687

688 **Acknowledgments**

689 Ibrahim MK was the recipient of a JSPS postdoctoral fellowship. This study was supported
690 by a Grant-In-Aid for JSPS Fellows (18F18098), and for Scientific Research (19K07586),
691 and grants from the Research Program on Hepatitis from the Japan Agency for Medical
692 Research and Development (AMED; 20fk0310104j0904, 19fk0310103j0303,
693 19fk0310109h0003, and 20fk0310109j0404). We gratefully acknowledge Dr Satoru
694 Kondo (Kanazawa University) for supplying us with Raji cells, Dr. Akihide Ryo (Yokohama

695 City University School of Medicine) for the kind gift of the anti-HBV core antibody, Miss
696 Yingfang Li, Dr. Tawfeek H Abdelhafez and Dr. Haruka Kudo (NIID) for technical support.
697

698 **Supplementary Materials**

699 **Plasmid Construction**

700 The reporter plasmid for the HBV core promoter mutant was generated by introducing two
701 point mutations (A1676C and C1678A) at the MafF binding site (Fig. 4A). Briefly, several
702 rounds of PCR amplification were performed using pGL4.10_Ce_xmut as the template; the
703 resulting products were digested with *HindIII* and *EcoRI* and subcloned into restriction-
704 digested pGL4.10 (Promega). The set of primers used in the construction of the mutated core
705 promoter include forward primers 5'-TCGAGGAATTCGGGTA CTTTACCACAGGAAC-
706 3' and 5'-CTTGACTCTCCGAAATGTCAACG-3' and reverse primers 5'-
707 TTGCCAAGCTTGAACATGAGATGATTAGGC-3' and
708 5'-CGTTGACATTTCCGGAGAGTCCAAG-3'. The sequence encoding HNF-4 α was
709 amplified from FR_HNF4A2 (Addgene; (68)) by PCR using primers including forward
710 primer, 5'-AGCTAGGATCCACCATGCGACTCTCCAAAACC-3' and reverse primer 5'-
711 GAGTCGAATTCTTACTTGTCGTCATCGTCTTTGTAGTCAGCAACTTGCCCAAAG
712 CG-3'. The resulting amplification product was cloned into pCDNA3.1 (Invitrogen) to yield
713 pcDNA3.1-HNF4A-FLAG. The reporter deletion mutant EnhII/CP Δ HNF-4 α #2 (Fig. 5A)
714 was constructed using pGL4.10_Ce_xmut as the template and a primer set including forward
715 primer 5'- TCGAGGGTACCGCCTGTAAATAGACCTATTG-3' and reverse primer 5'-
716 CTAACAAGCTTTCCTCCCCCAACTCCTCCC-3'; the amplification product was
717 subcloned into pGL4.10 using *HindIII* and *KpnI* restriction enzymes. All constructs were
718 validated by DNA sequencing. Plasmid DNAs used in transfection experiments were purified
719 using the Purelink Plasmid Midi Kit (Invitrogen).

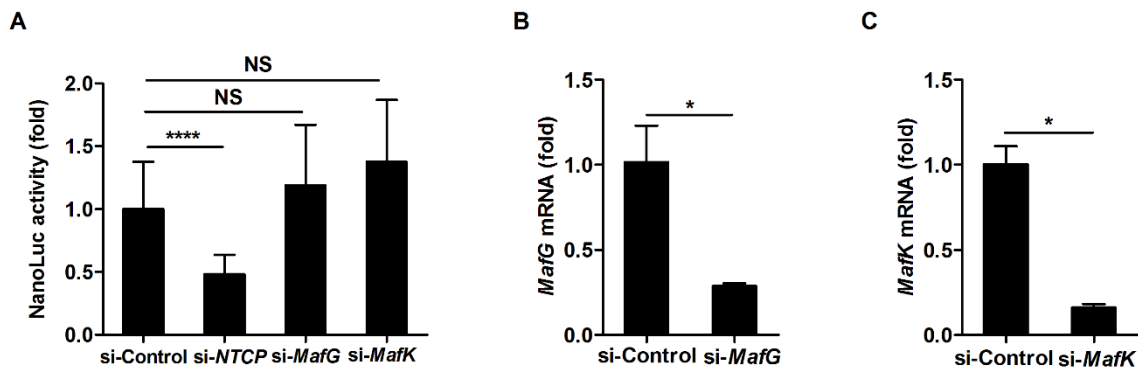
720 **Real-time PCR primers**

721 The relative levels of the *MafF*, *MafG*, and *MafK* mRNAs were determined using TaqMan
722 Gene Expression Assay primer-probe sets (Applied Biosystems) Hs05026540_g1,
723 Hs00536278_m1, and Hs00242747_m1, respectively; expression of *ACTB* (primer-probe set

724 Hs99999903_m1) was used as an internal control for normalization. The quantification of
725 pgRNA, *HNF-4 α* , and mRNAs encoding EBV BZLF1 and LMP1 was performed using
726 Power SYBR Green PCR Master Mix (Applied Biosystems); for these transcripts, expression
727 of *GAPDH* was used as an internal control for normalization. Data were expressed as fold
728 change relative to the mean of the control group. The set of primers used in these assays
729 included the Precore forward primer 5'-ACTGTTCAAGCCTCCAAGCTGT-3' and reverse
730 primer 5'-GAAGGCAAAAACGAGAGTAACTCCAC-3', *HNF-4 α* (69) forward primer 5'-
731 ACTACGGTGCCTCGAGCTGT-3' and reverse primer
732 5'-GGCACTGGTTCCTCTTGTCT-3'; *GAPDH* forward primer
733 5'-CTTTTGCGTGCCAG-3' and reverse primer 5'-TTGATGGCAACAATATCCAC-3',
734 EBV BZLF1 forward primer 5'-AAATTTAAGAGATCCTCGTGTAACATC-3' and
735 reverse primer 5'-CGCCTCCTGTTGAAGCAGAT-3', EBV LMP1 forward primer
736 5'-CTGGTTCCGGTGGAGATGA-3' and reverse primer
737 5'-CTGGTTCCGGTGGAGATGA-3'.

738

739 Supplementary Figure Legends

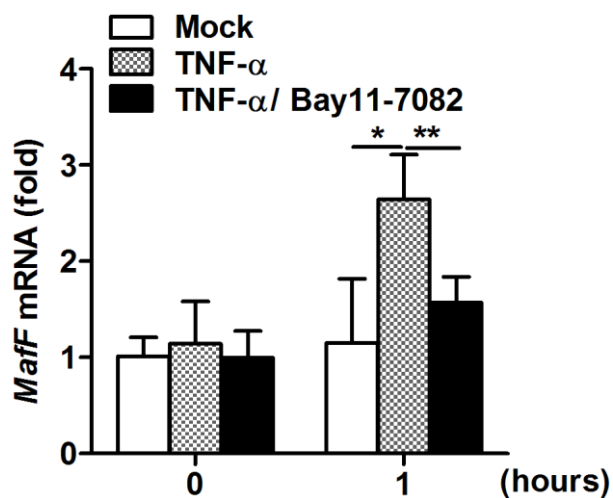


740

741 **Supplementary Figure 1. Silencing of *MafG* and *MafK* has no impact on HBV/NL. A.**

742 HepG2-hNTCP-C4 cells were transfected with control, *NTCP*, *MafG*, or *MafK*-targeting
743 siRNAs, followed two days later by infection with the HBV/NL reporter virus. At day 8 post-
744 infection, the cells were evaluated by luciferase assay; NanoLuc activity was determined and
745 plotted as fold differences relative to the mean luciferase activity of the control siRNA-

746 transfected cells. **B.–C.** HepG2 cells were transfected with control, *MafG*-targeting siRNA
747 (**B**), or *MafK*-targeting siRNA (**C**) for 2 days followed by the extraction of total RNA and
748 the quantification of the corresponding mRNAs. The data were normalized to the expression
749 of the *ACTB* and are presented as fold differences relative to the control siRNA-transfected
750 cells. All assays were performed in triplicate and include data from three independent
751 experiments. Data are presented as mean±SD; * $p<0.05$, **** $p<0.0001$; NS, not significant.
752



753

754 **Supplementary Figure 2. Induction of *MafF* mRNA in response to TNF- α is mediated**
755 **by NF- κ B signaling.** HepG2 cells were pretreated with Bay11-7082 or DMSO diluent
756 control for 1 h and then treated with 10 ng/ml TNF- α or left untreated (mock) for 1 h. Cells
757 were then lysed, total cellular RNA was extracted, and *MafF* mRNA was quantified by real-
758 time RT-PCR. The data were normalized to the expression of the *ACTB* and shown as the
759 fold change relative to the mean of the control group. All assays were performed in triplicate
760 include data from three independent experiments. Data are presented as mean±SD; * $p<0.05$,
761 ** $p<0.01$.

762

763 **References**

764 1. Orzalli MH, Knipe DM. Cellular sensing of viral DNA and viral evasion mechanisms. *Annu Rev*
765 *Microbiol.* 2014;68:477-92.

- 766 2. Chemudupati M, Kenney AD, Bonifati S, Zani A, McMichael TM, Wu L, et al. From APOBEC
767 to ZAP: Diverse mechanisms used by cellular restriction factors to inhibit virus infections. *Biochim*
768 *Biophys Acta Mol Cell Res.* 2019 Mar;1866(3):382-94.
- 769 3. Schoggins JW, MacDuff DA, Imanaka N, Gainey MD, Shrestha B, Eitson JL, et al. Pan-viral
770 specificity of IFN-induced genes reveals new roles for cGAS in innate immunity. *Nature.* 2014 Jan
771 30;505(7485):691-5.
- 772 4. Liang G, Liu G, Kitamura K, Wang Z, Chowdhury S, Monjurul AM, et al. TGF-beta suppression
773 of HBV RNA through AID-dependent recruitment of an RNA exosome complex. *PLoS Pathog.* 2015
774 Apr;11(4):e1004780.
- 775 5. Shiromoto F, Aly HH, Kudo H, Watashi K, Murayama A, Watanabe N, et al. IL-1beta/ATF3-
776 mediated induction of Ski2 expression enhances hepatitis B virus x mRNA degradation. *Biochem*
777 *Biophys Res Commun.* 2018 Sep 10;503(3):1854-60.
- 778 6. Amini-Bavil-Olyae S, Choi YJ, Lee JH, Shi M, Huang IC, Farzan M, et al. The antiviral effector
779 IFITM3 disrupts intracellular cholesterol homeostasis to block viral entry. *Cell Host Microbe.* 2013
780 Apr 17;13(4):452-64.
- 781 7. Wustenhagen E, Boukhallouk F, Negwer I, Rajalingam K, Stubenrauch F, Florin L. The Myb-
782 related protein MYPOP is a novel intrinsic host restriction factor of oncogenic human
783 papillomaviruses. *Oncogene.* 2018 Nov;37(48):6275-84.
- 784 8. Aly HH, Suzuki J, Watashi K, Chayama K, Hoshino S, Hijikata M, et al. RNA Exosome Complex
785 Regulates Stability of the Hepatitis B Virus X-mRNA Transcript in a Non-stop-mediated (NSD) RNA
786 Quality Control Mechanism. *J Biol Chem.* 2016 Jul 29;291(31):15958-74.
- 787 9. Meurs EF, Watanabe Y, Kadereit S, Barber GN, Katze MG, Chong K, et al. Constitutive
788 expression of human double-stranded RNA-activated p68 kinase in murine cells mediates
789 phosphorylation of eukaryotic initiation factor 2 and partial resistance to encephalomyocarditis
790 virus growth. *J Virol.* 1992 Oct;66(10):5805-14.
- 791 10. Meyerson NR, Zhou L, Guo YR, Zhao C, Tao YJ, Krug RM, et al. Nuclear TRIM25 Specifically
792 Targets Influenza Virus Ribonucleoproteins to Block the Onset of RNA Chain Elongation. *Cell Host*
793 *Microbe.* 2017 Nov 8;22(5):627-38 e7.
- 794 11. Chen G, Liu CH, Zhou L, Krug RM. Cellular DDX21 RNA helicase inhibits influenza A virus
795 replication but is counteracted by the viral NS1 protein. *Cell Host Microbe.* 2014 Apr 9;15(4):484-93.
- 796 12. Nassal M. HBV cccDNA: viral persistence reservoir and key obstacle for a cure of chronic
797 hepatitis B. *Gut.* 2015 Dec;64(12):1972-84.
- 798 13. Krause-Kyora B, Susat J, Key FM, Kuhnert D, Bosse E, Immel A, et al. Neolithic and medieval
799 virus genomes reveal complex evolution of hepatitis B. *Elife.* 2018 May 10;7.
- 800 14. Wieland S, Thimme R, Purcell RH, Chisari FV. Genomic analysis of the host response to
801 hepatitis B virus infection. *Proc Natl Acad Sci U S A.* 2004 Apr 27;101(17):6669-74.
- 802 15. Katsuoka F, Yamamoto M. Small Maf proteins (MafF, MafG, MafK): History, structure and
803 function. *Gene.* 2016 Jul 25;586(2):197-205.
- 804 16. Kannan MB, Solovieva V, Blank V. The small MAF transcription factors MAFF, MAFG and
805 MAFK: current knowledge and perspectives. *Biochim Biophys Acta.* 2012 Oct;1823(10):1841-6.
- 806 17. Massrieh W, Derjuga A, Doualla-Bell F, Ku CY, Sanborn BM, Blank V. Regulation of the MAFF
807 transcription factor by proinflammatory cytokines in myometrial cells. *Biol Reprod.* 2006
808 Apr;74(4):699-705.
- 809 18. Hau PM, Lung HL, Wu M, Tsang CM, Wong KL, Mak NK, et al. Targeting Epstein-Barr Virus in
810 Nasopharyngeal Carcinoma. *Front Oncol.* 2020;10:600.

- 811 19. Nishitsuji H, Ujino S, Shimizu Y, Harada K, Zhang J, Sugiyama M, et al. Novel reporter system
812 to monitor early stages of the hepatitis B virus life cycle. *Cancer Sci.* 2015 Nov;106(11):1616-24.
- 813 20. Iwamoto M, Watashi K, Tsukuda S, Aly HH, Fukasawa M, Fujimoto A, et al. Evaluation and
814 identification of hepatitis B virus entry inhibitors using HepG2 cells overexpressing a membrane
815 transporter NTCP. *Biochem Biophys Res Commun.* 2014 Jan 17;443(3):808-13.
- 816 21. Bartenschlager R, Schaller H. Hepadnaviral assembly is initiated by polymerase binding to
817 the encapsidation signal in the viral RNA genome. *EMBO J.* 1992 Sep;11(9):3413-20.
- 818 22. Hirsch RC, Lavine JE, Chang LJ, Varmus HE, Ganem D. Polymerase gene products of hepatitis
819 B viruses are required for genomic RNA packaging as well as for reverse transcription. *Nature.* 1990
820 Apr 5;344(6266):552-5.
- 821 23. Sandelin A, Alkema W, Engstrom P, Wasserman WW, Lenhard B. JASPAR: an open-access
822 database for eukaryotic transcription factor binding profiles. *Nucleic Acids Res.* 2004 Jan
823 1;32(Database issue):D91-4.
- 824 24. Yu X, Mertz JE. Differential regulation of the pre-C and pregenomic promoters of human
825 hepatitis B virus by members of the nuclear receptor superfamily. *J Virol.* 1997 Dec;71(12):9366-74.
- 826 25. Lopez-Cabrera M, Letovsky J, Hu KQ, Siddiqui A. Transcriptional factor C/EBP binds to and
827 transactivates the enhancer element II of the hepatitis B virus. *Virology.* 1991 Aug;183(2):825-9.
- 828 26. Raney AK, Johnson JL, Palmer CN, McLachlan A. Members of the nuclear receptor
829 superfamily regulate transcription from the hepatitis B virus nucleocapsid promoter. *J Virol.* 1997
830 Feb;71(2):1058-71.
- 831 27. Gilbert S, Galarneau L, Lamontagne A, Roy S, Belanger L. The hepatitis B virus core promoter
832 is strongly activated by the liver nuclear receptor fetoprotein transcription factor or by ectopically
833 expressed steroidogenic factor 1. *J Virol.* 2000 Jun;74(11):5032-9.
- 834 28. Zhou W, Ma Y, Zhang J, Hu J, Zhang M, Wang Y, et al. Predictive model for inflammation
835 grades of chronic hepatitis B: Large-scale analysis of clinical parameters and gene expressions. *Liver
836 Int.* 2017 Nov;37(11):1632-41.
- 837 29. Speck SH, Chatila T, Flemington E. Reactivation of Epstein-Barr virus: regulation and function
838 of the BZLF1 gene. *Trends Microbiol.* 1997 Oct;5(10):399-405.
- 839 30. Li H, Liu S, Hu J, Luo X, Li N, A MB, et al. Epstein-Barr virus lytic reactivation regulation and
840 its pathogenic role in carcinogenesis. *Int J Biol Sci.* 2016;12(11):1309-18.
- 841 31. Murata T, Narita Y, Sugimoto A, Kawashima D, Kanda T, Tsurumi T. Contribution of myocyte
842 enhancer factor 2 family transcription factors to BZLF1 expression in Epstein-Barr virus reactivation
843 from latency. *J Virol.* 2013 Sep;87(18):10148-62.
- 844 32. Kurokawa H, Motohashi H, Sueno S, Kimura M, Takagawa H, Kanno Y, et al. Structural basis
845 of alternative DNA recognition by Maf transcription factors. *Mol Cell Biol.* 2009 Dec;29(23):6232-44.
- 846 33. Schreiner S, Kinkley S, Burck C, Mund A, Wimmer P, Schubert T, et al. SPOC1-mediated
847 antiviral host cell response is antagonized early in human adenovirus type 5 infection. *PLoS Pathog.*
848 2013;9(11):e1003775.
- 849 34. Kataoka K, Igarashi K, Itoh K, Fujiwara KT, Noda M, Yamamoto M, et al. Small Maf proteins
850 heterodimerize with Fos and may act as competitive repressors of the NF-E2 transcription factor.
851 *Mol Cell Biol.* 1995 Apr;15(4):2180-90.
- 852 35. Fujiwara KT, Kataoka K, Nishizawa M. Two new members of the maf oncogene family, mafK
853 and mafF, encode nuclear b-Zip proteins lacking putative trans-activator domain. *Oncogene.* 1993
854 Sep;8(9):2371-80.

- 855 36. Kerppola TK, Curran T. A conserved region adjacent to the basic domain is required for
856 recognition of an extended DNA binding site by Maf/Nrl family proteins. *Oncogene*. 1994
857 Nov;9(11):3149-58.
- 858 37. Kataoka K, Noda M, Nishizawa M. Maf nuclear oncoprotein recognizes sequences related to
859 an AP-1 site and forms heterodimers with both Fos and Jun. *Mol Cell Biol*. 1994 Jan;14(1):700-12.
- 860 38. Ney PA, Sorrentino BP, Lowrey CH, Nienhuis AW. Inducibility of the HS II enhancer depends
861 on binding of an erythroid specific nuclear protein. *Nucleic acids research*. 1990 Oct 25;18(20):6011-
862 7.
- 863 39. Rushmore TH, Morton MR, Pickett CB. The antioxidant responsive element. Activation by
864 oxidative stress and identification of the DNA consensus sequence required for functional activity.
865 *The Journal of biological chemistry*. 1991 Jun 25;266(18):11632-9.
- 866 40. Kimura M, Yamamoto T, Zhang J, Itoh K, Kyo M, Kamiya T, et al. Molecular basis
867 distinguishing the DNA binding profile of Nrf2-Maf heterodimer from that of Maf homodimer. *The*
868 *Journal of biological chemistry*. [Research Support, Non-U.S. Gov't]. 2007 Nov 16;282(46):33681-90.
- 869 41. Motohashi H, O'Connor T, Katsuoka F, Engel JD, Yamamoto M. Integration and diversity of
870 the regulatory network composed of Maf and CNC families of transcription factors. *Gene*. 2002 Jul
871 10;294(1-2):1-12.
- 872 42. Motohashi H, Katsuoka F, Shavit JA, Engel JD, Yamamoto M. Positive or negative MARE-
873 dependent transcriptional regulation is determined by the abundance of small Maf proteins. *Cell*.
874 2000 Dec 8;103(6):865-75.
- 875 43. Kataoka K, Nishizawa M, Kawai S. Structure-function analysis of the maf oncogene product,
876 a member of the b-Zip protein family. *Journal of Virology*. 1993;67(4):2133-41.
- 877 44. Motohashi H, Shavit JA, Igarashi K, Yamamoto M, Engel JD. The world according to Maf.
878 *Nucleic Acids Res*. 1997 Aug 1;25(15):2953-59.
- 879 45. Liu T, Zhang L, Joo D, Sun SC. NF-kappaB signaling in inflammation. *Signal Transduct Target*
880 *Ther*. 2017;2.
- 881 46. Migita K, Maeda Y, Abiru S, Nakamura M, Komori A, Miyazoe S, et al. Polymorphisms of
882 interleukin-1beta in Japanese patients with hepatitis B virus infection. *J Hepatol*. 2007
883 Mar;46(3):381-6.
- 884 47. Gonzalez-Amaro R, Garcia-Monzon C, Garcia-Buey L, Moreno-Otero R, Alonso JL, Yague E,
885 et al. Induction of tumor necrosis factor alpha production by human hepatocytes in chronic viral
886 hepatitis. *J Exp Med*. 1994 Mar 1;179(3):841-8.
- 887 48. Xia Y, Stadler D, Lucifora J, Reisinger F, Webb D, Hosel M, et al. Interferon-gamma and Tumor
888 Necrosis Factor-alpha Produced by T Cells Reduce the HBV Persistence Form, cccDNA, Without
889 Cytolysis. *Gastroenterology*. 2016 Jan;150(1):194-205.
- 890 49. Park YK, Park ES, Kim DH, Ahn SH, Park SH, Lee AR, et al. Cleaved c-FLIP mediates the antiviral
891 effect of TNF-alpha against hepatitis B virus by dysregulating hepatocyte nuclear factors. *Journal of*
892 *hepatology*. [Research Support, Non-U.S. Gov't]. 2016 Feb;64(2):268-77.
- 893 50. Quarleri J. Core promoter: a critical region where the hepatitis B virus makes decisions.
894 *World journal of gastroenterology*. [Review]. 2014 Jan 14;20(2):425-35.
- 895 51. Ishida H, Ueda K, Ohkawa K, Kanazawa Y, Hosui A, Nakanishi F, et al. Identification of
896 multiple transcription factors, HLF, FTF, and E4BP4, controlling hepatitis B virus enhancer II. *Journal*
897 *of virology*. 2000 Feb;74(3):1241-51.
- 898 52. Moolla N, Kew M, Arbuthnot P. Regulatory elements of hepatitis B virus transcription.
899 *Journal of viral hepatitis*. [Research Support, Non-U.S. Gov't

- 900 Review]. 2002 Sep;9(5):323-31.
- 901 53. Abraham TM, Loeb DD. The topology of hepatitis B virus pregenomic RNA promotes its
902 replication. *J Virol.* 2007 Nov;81(21):11577-84.
- 903 54. Mitra B, Wang J, Kim ES, Mao R, Dong M, Liu Y, et al. Hepatitis B Virus Precore Protein p22
904 Inhibits Alpha Interferon Signaling by Blocking STAT Nuclear Translocation. *J Virol.* 2019 Jul 1;93(13).
- 905 55. Yu Y, Wan P, Cao Y, Zhang W, Chen J, Tan L, et al. Hepatitis B Virus e Antigen Activates the
906 Suppressor of Cytokine Signaling 2 to Repress Interferon Action. *Sci Rep.* 2017 May 11;7(1):1729.
- 907 56. Wang Y, Cui L, Yang G, Zhan J, Guo L, Chen Y, et al. Hepatitis B e Antigen Inhibits NF-kappaB
908 Activity by Interrupting K63-Linked Ubiquitination of NEMO. *J Virol.* 2019 Jan 15;93(2).
- 909 57. Morrison TE, Kenney SC. BZLF1, an Epstein-Barr virus immediate-early protein, induces p65
910 nuclear translocation while inhibiting p65 transcriptional function. *Virology.* 2004 Oct
911 25;328(2):219-32.
- 912 58. Ishida Y, Yamasaki C, Yanagi A, Yoshizane Y, Fujikawa K, Watashi K, et al. Novel robust in
913 vitro hepatitis B virus infection model using fresh human hepatocytes isolated from humanized mice.
914 *The American journal of pathology.* [Research Support, Non-U.S. Gov't]. 2015 May;185(5):1275-85.
- 915 59. Zhu Q, Zhang M, Shi M, Liu Y, Zhao Q, Wang W, et al. Human B cells have an active phagocytic
916 capability and undergo immune activation upon phagocytosis of *Mycobacterium tuberculosis*.
917 *Immunobiology.* [Research Support, Non-U.S. Gov't]. 2016 Apr;221(4):558-67.
- 918 60. Wang H, Kim S, Ryu WS. DDX3 DEAD-Box RNA helicase inhibits hepatitis B virus reverse
919 transcription by incorporation into nucleocapsids. *J Virol.* 2009 Jun;83(11):5815-24.
- 920 61. Sugiyama M, Tanaka Y, Kato T, Orito E, Ito K, Acharya SK, et al. Influence of hepatitis B virus
921 genotypes on the intra- and extracellular expression of viral DNA and antigens. *Hepatology.* 2006
922 Oct;44(4):915-24.
- 923 62. Lena Allweiss MY, Barbara Testoni, Julie Lucifora, Chunkyu Ko, Bingqian Qu, Dieter Glebe,
924 Elena S. kim, Mark Lutgehetmann, Stephan Urban, Guofeng Cheng, William Delaney, Massimo
925 Levrero, Ulrike Protzer, Fabien Zoulim, Haitao Guo, Maura Dandri. Final results of the concerted
926 harmonization efforts for HBV cccDNA quantification. 2019 International HBV Meeting, Melbourne,
927 Australia2019.
- 928 63. Qu B, Ni Y, Lempp FA, Vondran FWR, Urban S. T5 Exonuclease Hydrolysis of Hepatitis B Virus
929 Replicative Intermediates Allows Reliable Quantification and Fast Drug Efficacy Testing of Covalently
930 Closed Circular DNA by PCR. *Journal of virology.* [Research Support, Non-U.S. Gov't]. 2018 Dec
931 1;92(23).
- 932 64. Deng L, Gan X, Ito M, Chen M, Aly HH, Matsui C, et al. Peroxiredoxin 1, a Novel HBx-
933 Interacting Protein, Interacts with Exosome Component 5 and Negatively Regulates Hepatitis B Virus
934 (HBV) Propagation through Degradation of HBV RNA. *J Virol.* 2019 Mar 15;93(6).
- 935 65. Murata T, Sato Y, Nakayama S, Kudoh A, Iwahori S, Isomura H, et al. TORC2, a coactivator of
936 cAMP-response element-binding protein, promotes Epstein-Barr virus reactivation from latency
937 through interaction with viral BZLF1 protein. *The Journal of biological chemistry.* [Research Support,
938 Non-U.S. Gov't]. 2009 Mar 20;284(12):8033-41.
- 939 66. Sakurai F, Mitani S, Yamamoto T, Takayama K, Tachibana M, Watashi K, et al. Human
940 induced-pluripotent stem cell-derived hepatocyte-like cells as an in vitro model of human hepatitis
941 B virus infection. *Scientific reports.* [Research Support, Non-U.S. Gov't]. 2017 Apr 4;7:45698.
- 942 67. Watashi K, Liang G, Iwamoto M, Marusawa H, Uchida N, Daito T, et al. Interleukin-1 and
943 tumor necrosis factor-alpha trigger restriction of hepatitis B virus infection via a cytidine deaminase
944 activation-induced cytidine deaminase (AID). *J Biol Chem.* 2013 Nov 1;288(44):31715-27.

- 945 68. Thomas H, Senkel S, Erdmann S, Arndt T, Turan G, Klein-Hitpass L, et al. Pattern of genes
946 influenced by conditional expression of the transcription factors HNF6, HNF4alpha and HNF1beta in
947 a pancreatic beta-cell line. *Nucleic Acids Res.* 2004 Nov 1;32(19):e150.
- 948 69. Sambathkumar R, Akkerman R, Dastidar S, Roelandt P, Kumar M, Bajaj M, et al. Generation
949 of hepatocyte- and endocrine pancreatic-like cells from human induced endodermal progenitor cells.
950 *PLoS one.* [Research Support, Non-U.S. Gov't]. 2018;13(5):e0197046.

951

952